HIGH PERFORMANCE CAST ALUMINIUM ALLOYS FOR AUTOMOTIVE APPLICATIONS

M.Tech. Thesis

By
REETURAJ TAMULY
(1802105023)

DISCIPLINE OF METALLURGY ENGINEERING AND MATERIAL SCIENCE
INDIAN INSTITUTE OF TECHNOLOGY INDORE

JUNE 2020

HIGH PERFORMANCE CAST ALUMINIUM ALLOYS FOR AUTOMOTIVE APPLICATIONS

A THESIS

Submitted in partial fulfillment of the requirements for the award of the degree
of
Master of Technology

by
REETURAJ TAMULY
(1802105023)

DISCIPLINE OF METALLURGY ENGINEERING AND MATERIAL SCIENCE
INDIAN INSTITUTE OF TECHNOLOGY INDORE
JUNE 2020

INDIAN INSTITUTE OF TECHNOLOGY INDORE

CANDIDATE'S DECLARATION

I hereby certify that the work which is being presented in the thesis entitled **HIGH PERFORMANCE CAST ALUMINIUM ALLOYS FOR AUTOMOTIVE APPLICATIONS** in the partial fulfillment of the requirements for the award of the degree of **MASTER OF TECHNOLOGY** and submitted in the **DISCIPLINE OF METALLURGY ENGINEERING AND MATERIAL SCIENCE, Indian Institute of Technology Indore**, is an authentic record of my own work carried out during the time period from July, 2019 to June,2020 under the supervision of Dr. Hemant Borkar, Assiatant Professor, Department of Metallurgy Engineering and Material Science, IIT Indore

The matter presented in this thesis has not been submitted by me for the award of any other degree of this or any other institute.

19.06.2020

Signature of the student with date
REETURAJ TAMULY

This is to certify that the above statement made by the candidate is correct to the best of my/our knowledge.

19.06.2020

Signature of the Supervisor of
M.Tech. thesis #1 (with date)
Dr. HEMANT BORKAR
(NAME OF SUPERVISOR)

19.06.2020

Signature of the Supervisor of
M.Tech. thesis #2 (with date)

REETURAJ TAMULY has successfully given his/her M.Tech. Oral Examination held on **24.06.2020**.

Signature(s) of Supervisor(s) of M.Tech. thesis
Date: 28.06.2020

Convener, DPGC
Date:

Signature of PSPC Member #1
Date: 29.06.2020

Signature of PSPC Member #1
Date:

ACKNOWLEDGEMENTS

First of all, I would like to express my deep sense of gratitude to Dr, Hemant Borkar, Assistant Professor of Metallurgy Engineering and Material Science Department, IIT Indore for giving me an opportunity to work under his supervision. I would also like to thank him for his continuous support and motivation during my research work.

I am also grateful to Dr. Eswara Prasad Korimilli, Assistant Professor of Metallurgy Engineering and Material Science Department, IIT Indore and Dr. Sumanta Samal, Assistant Professor of Metallurgy Engineering and Material Science Department, IIT Indore for periodic evaluation of my research progress and for their valuable comments and advices.

I would also extend my sincere gratitude to Mr Amit Behl, Quality Control Manager, Hero MotoCorp Ltd. for providing industrial support and guidance.

Finally, I would like to thank my lab mates, MEMS department staff of IIT Indore for their inspiration and help and providing me all the laboratory facilities during the period of research work.

ABSTRACT

Al-Si alloy of grade A356 is widely used in several industries such as automobile, aerospace , defence and others due to its lighter weight, high strength, excellent castability, excellent thermal conductivity, corrosion resistance, wear/abrasive resistance and other excellent mechanical properties. A356 alloy castings are used to manufacture aircraft parts, machine parts, truck chassis parts and structural parts which require high strength. Here we investigate the effect of squeeze casting and functioning of various master alloys, that are used to either grain refine the α-Al matrix or cause modification of Si morphology to improve the microstructural and wear properties like fretting wear and dry sliding wear of the Al-Si alloy. The most commercially used master alloys are Al-Ti-B alloy which act as a grain refiner and Al-Sr alloy which act as a modifier. To achieve better results, a combination of both grain refiner and modifiers is used to achieve fine α-Al phase and fine fibrous like Si particle morphology. However, as per previous research work it was investigated that the combination of Al-Ti-B alloy and Al-Sr alloy may cause a poisoning effect due to the reaction between Sr and B, which in turn reduces the modification ability of Sr. Hence in this research work, an attempt was made to find out an optimum amount of both of these master alloys that should be used to obtain better results in terms of microstructural refinement, modification of morphology of Si particles and other intermetallic phases and improvement in mechanical properties like hardness and wear properties. A combination of 750ppm of Ti and 150ppm of B added in the form of Al-5Ti-1B master alloy and about 200ppm of Sr added in the form of Al-10Sr master alloy to squeeze cast A356 alloy, showed significant improvement in hardness and wear properties of the alloy due to refinement of grain size and change in the morphology of Si and other iron based intermetallics.. Moreover, the process of squeeze casting under a pressure of 200MPa, also improved the wear properties of the alloy due to reduction in porosities, decrease in secondary dendrite arm spacings and modification of Si morphology.

However, the combination of 750ppm of Ti, 150ppm of B added in the form of Al-5Ti-1B and 300ppm of Sr added in the form of Al-10Sr to squeeze cast A356 alloy, did not show much improvement in the wear properties of the alloy. Further investigation is required for more conclusive results.

LIST OF PUBLICATIONS

1. **Effect of squeeze casting on microstructure and wear properties of A356 alloy**
   Authors: Reeturaj Tamuly, Mr Amit Behl, Dr. Hemant Borkar
   International Conference on Advance Light Weight Materials and Structures, March 2020
   Organised by CMR Technical Campus, Hyderabad
   Publication Type: Springer Nature
   Status: Accepted

2. **Effect of grain refiner and modifier on microstructure and wear properties of squeeze cast Si based Al alloy**
   Authors: Reeturaj Tamuly, Mr Amit Behl, Dr. Hemant Borkar
   Status: To be submitted soon to a suitable Journal

TABLE OF CONTENTS

LIST OF FIGURES

LIST OF TABLES

ACRONYMS

Acronym	Meaning
SDAS	Secondary Dendrite Arm Spacing
SEM	Scanning Electron Microscope
EDS	Energy Dispersive X-Ray Spectroscopy
BSE	Back Scattered Electrons
XRD	X-Ray Diffraction
SV	Sliding Velocity
COF	Coefficient Of Friction
WTD	Wear Track Diameter

Chapter 1

Introduction

1.1 Background

Lightweight metals have recently received increasing attention for automotive applications due to their potential to reduce the weight of vehicles thereby reducing environmental impact. Among all the light weight metals, Al is widely used engineering material due to its excellent corrosion resistivity, low electrical resistivity and high thermal conductivity. Al alloys can be subdivided into cast and wrought alloys depending upon the type of fabrication performed. For high temperature automotive applications, cast Al alloys are majorly utilized due to their favourable characteristics like negligible gas solubility other than hydrogen, smooth surface finish and relatively low melting temperature. Generally, Si based Al alloys are widely used to manufacture automobile components which work at both ambient and elevated temperature (upto 200°C) due to outstanding characteristics like low manufacturing cost, high strength to weight ratio, recyclability and castability. Copper and Magnesium are commonly used as alloying elements to improve mechanical properties at both ambient and high temperatures and also to make heat treatment possible. The microstructure of these alloys consists of α-Al dendrites as the major constituent, followed by eutectic Si particles in the interdendritic regions. Many intermetallic phases like Al_2Cu, Mg_2Si, iron bearing phases etc are also present in the alloy. The dendritic arm spacings, grain size, morphology of Si particles, morphology of intermetallic phases and their distribution govern the mechanical properties of such casting alloys. It is observed that the refinement and modification of microstructure improve the tensile properties of the alloy. The refinement of the microstructure can be obtained by increasing rate of cooling or chemical or mechanical modification. It is reported that application of Al-Si-Cu-Mg alloys beyond a temperature around 230°C leads to coarsening of Si particles and Cu and Mg bearing phases get dissolved.

1.2 Alloying elements

Among all the Al alloys, the most popular cast Al alloys widely used in industries are Si based Al alloys. Si being the major alloying element improves fluidity which helps in production of components of complex shape. Moreover, addition of Si increases the ability to resist corrosion, reduces coefficient of thermal expansion, increases wear/abrasive resistant property, improve castability and machinability of the alloy, increases the specific strength and also makes the alloy heat treatable.

Si based Al alloy are widely used in aircraft industries, automobile applications and so on. It is a binary eutectic alloy with a composition and temperature of 12.6 wt. % Si and 577°C respectively at a eutectic point. The maximum solubility limit of Si in Al is 1.6 wt. %, whereas the solubility of Al in Si is almost negligible. In hypoeutectic alloys, Al solidifies first in the form of dendrites and then grow in <100> direction. The solidified structure of an as cast Al-Si alloy of grade A356, which is a hypoeutectic alloy of 7 wt. % Si, has a coarse α-Al dendritic matrix phase and its inter-dendritic regions are occupied by needle/acicular or plate-like morphology of pure Si particles in eutectic with Al. These inter-dendritic regions are also known as Al-Si eutectic regions. Hypo-eutectic alloys have a α-Al phase which is soft and ductile and a eutectic Si phase which is hard and brittle whereas in hyper-eutectic alloys, Si particles are coarse and angular shaped and also contain eutectic Si phase. The Al-Si phase diagram is shown in Fig. 1.

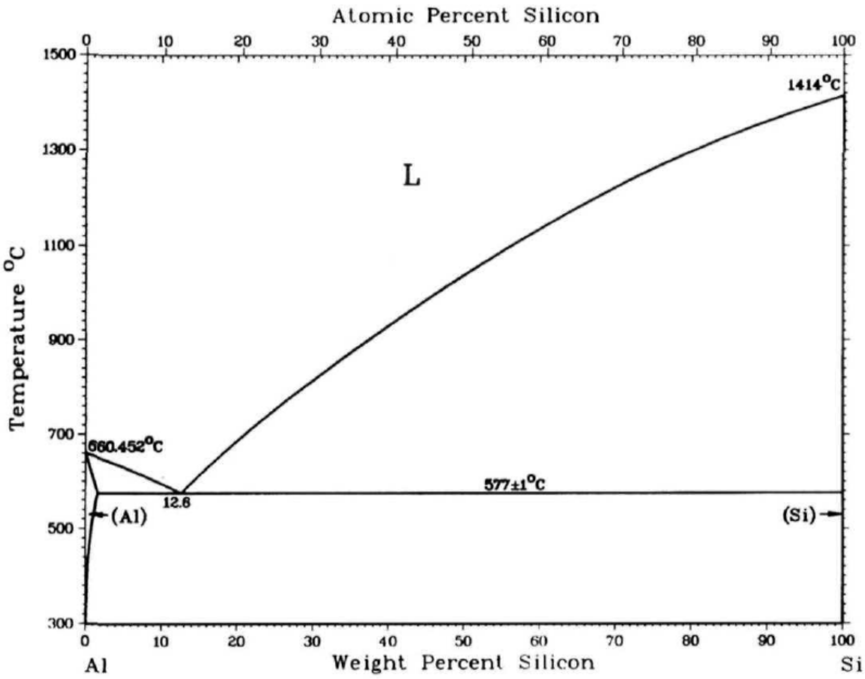

Figure 1. Aluminium Silicon phase diagram. (ASM specialty hand book: Aluminium and Aluminium alloys [1])

Other alloying elements like Cu, Fe and Mg added to Al-Si alloy form intermetallic compounds. Some of the common intermetallic compounds are Mg_2Si, Al_2Cu, α-$Al_{15}(Fe,Mn)_3Si_2$ and β-Al_5FeSi. Mondolfo et al, Haizhi Ye, Eklund JE, Taylor JA et al and Suarez Pena B et al reported that β-Fe bearing phases are undesirable for mechanical properties due to its needle shape morphology [2-6]. Hence modifiers such as Na, Sr, Sb etc are used to modify the morphology [7-10]. α phase intermetallic are found in the form of blocky shaped particles and "Chinese Script" morphology and are not detrimental to mechanical properties.

Magnesium as an alloying element, improve the tensile properties of Al-Si alloy at elevated temperature upto ~ 200°C. Mg also enhances resistance to creep and reduces the loss of strength at elevated temperature. The increase in strength at elevated temperature is obtained after solutionising treatment due to activation of precipitates of Mg bearing phases leading to precipitation hardening. This increase in strength at elevated temperature is due to the precipitation of β- Mg_2Si

precipitates [11-13]. Similarly, addition of Cu also increase strength and creep resistant property of Al-Si alloys by precipitation of θ-Al_2Cu precipitates. However, there are some transition phases like GP zones, θ', θ" in case of Cu bearing phases which also enhance the properties of the alloy [14,15].

The coarse, acicular or needle shaped morphology of Si particle act as stress concentration sites and hence deteriorate the properties of the alloy. Hence to improve mechanical properties like tensile strength, hardness, fracture toughness, wear properties etc., the alloy must undergo grain refinement or modification or combination of both. This can be achieved with the help of mechanical modification like squeeze casting, which is a combined process of forging and casting operation, and chemical modification like addition of master alloys like grain refiner and grain modifier.

1.3 Classification of Aluminium alloys

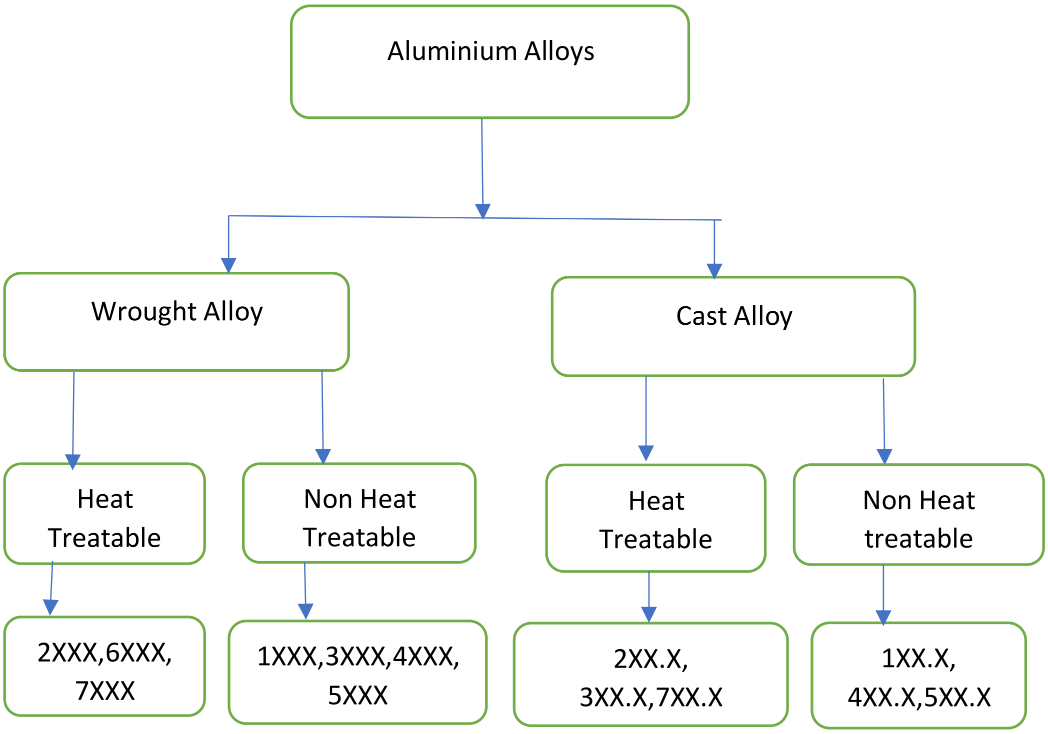

1.4 Designation of cast Al alloy

As per American Aluminium Association (AAA), cast Al alloys are designated as described below.

Let us consider a cast Al alloy of grade : **Z 3XX.YV**

Z →Optional Registration Code

First Version has no letter, Second Version is AXXX, third is BXXX ,etc., in order of registration, by itself tells us nothing else.

3 →General Family

XX →Member within the family

Y →Specimen of :

XXX.0 is casting composition

XXX.1 is Ingot

XXX.2 is High purity ingot

V →Modification code:

XXX.XS is 0.005-0.08%Sr

XXX.XC is 0.008-0.15%C

XXX.XP is 0.06%P

1.5 Casting defects

The melting conditions, the process of manufacturing and treatments after solidification adversely affect the microstructure by generation of various types of defects in Al-Si alloy castings. These defects degrade the mechanical properties and lower the performance of the product.

Lowering the defects makes it easier to design thin sections, reduce the weight and produce reliable cast products. Defects in Al-Si alloys arise during processing or due to chemical composition, formation of oxides and gas porosities are most common casting defects which are due to poor treatment of alloy melt. High iron content also leads to the formation of undesirable β compounds which adversely affect the mechanical properties.

Hydrogen is not soluble in solid state and hence wants to escape to the atmosphere after the solidification of the melt. If it is unable to escape from the solidified product, it form pores within the castings called as gas porosities which deteriorate the properties of the alloy.

When the melt is exposed to oxygen, Al form a layer of oxide on the surface. If the layer of oxide film is removed, another layer of oxide will form immediately. The oxide layer on Al has amorphous structure which has low permeability and hence acts as protective layer on the liquid Al surface. There is no threat to the quality of liquid metal as long as the oxide layer is present on liquid Al surface. But on pouring and transforming of molten metal will introduce new oxide film onto the melt which appear as defects in the cast product.

Other than oxides and gas porosities, presence of iron deteriorate the properties of Si based Al alloys. The solubility of Fe in Al is 0.05 wt % at 660°C. At room temperature, the solubility of Fe in Al is even low. Iron in melt condition forms β-intermetallic compounds which are detrimental to mechanical properties. Higher the Fe content, lower is the ductility of the alloy. However, a small amount of Fe about 0.8-1 wt % is favourable, in order to prevent die soldering.

Intermetallic phases like α-Fe, β-Fe bearing phases are observed in Al-Si alloys. The α-phases are identified as Chinese script morphology or polyhedron and β-phase needles are identified as two-dimensional needles and three dimensional platelets. The β-phase morphology is detrimental to mechanical properties. Hence, the formation of α-phase can be promoted by addition of Mn in order to neutralise the formation of β-phase [16].

Chapter 2

Review of past work and problem formulation

2.1 Squeeze casting

Squeeze casting is a pressure assisted process in which liguid metal is solidified under the application of high pressure. It was first demonstrated in Russia where the liquid metal was solidified/casted under the effect of steam pressure [17]. However, the first attempt of squeeze casting on Al-Si alloy was made by Welter in 1931 [18]. Squeeze casting is also termed as squeeze forming or liquid metal forging or extrusion casting. The major benefits of squeeze casting are to prevent gas porosities or shrinkage porosities, reduce grain size, reduce solidification cracks and many more.

Some of the previous work done by eminent researchers are discussed here. Chatterjee and Das worked on a simple squeeze casting apparatus to find out the effect of pressure on Si based Al alloy of grade LM6 having 12.7 wt.% Si [19,20]. They observed that there is significant rise in mechanical properties under the effect of pressure. This was due to the shifting of eutectic composition towards Si rich end in the binary phase diagram of the alloy system (as primary α-Al phase increases), decrease in dendritic arm spacing and refinement of eutectics.

Chadwick and Yue worked on heat treatable alloys like LM24/A380 (Al-Si8Cu3Fe) and LM25/A357 (AlSi7Mg) [21]. They observed that the yield strength and UTS increase upon squeeze casting. LM24 alloy when squeeze cast and heat-treated showed improvement in mechanical properties than that of conventionally cast LM25 alloy.

Dong et al examined the effects of Sr and Fe on LM25 alloy when processed by squeeze casting process [22]. They compared squeeze casting with gravity die casting process. The yield strength of the samples cast by gravity die casting were found to be higher than that of squeeze casting. The heat treated samples under T6 condition showed equal yield strengths in both the cases. The ultimate tensile strength of squeeze cast samples was found to be higher than that of gravity cast samples in both as-cast and heat treatment conditions. Reduction in porosity and refinement in Fe bearing phases was found in squeeze cast samples. Ductility got improved in both as-cast with and without heat treatment samples due to modification of Al-Fe-Si particles from needle shaped β-Al_5FeSi to a Chinese script morphology. Addition of Sr did not affect the morphology of eutectic Si particles.

Chadwick and Yue worked on Al-7Si and Al-14Si binary alloy system [21]. Squeeze casting process altered the microstructure due to high coefficient of heat transfer between die and melt resulting high pressure during casting. High casting pressure also increases liquidus temperature and eutectic point of the alloy.

Okada et al examined the effect of squeeze casting in Al-Si with 20 wt.% Si alloy system [23]. He found that with increase in squeeze pressure, the density of Al-Si alloy increases to a maximum at some critical pressure and then does not show any further increase in density beyond this critical point. He concluded that with increase in Si content the critical pressure increases.

Hence it can be concluded that, with increase in squeeze pressure, during squeeze casting process, following advantages were obtained:

- Increase in UTS and yield strength
- Modification of eutectic Si morphology
- Refinement of deleterious intermetallic
- Improvement in metal to die heat transfer

2.2 Cooling rate refinement and mechanisms

In hypoeutectic Al-Si alloy, the primary Al phase undergo solidification in dendritic manner followed by growth of secondary arms around the primary stem. The undercooling mainly depends upon the cooling rate, the concentration of alloying element and the type of alloying elements in the melt. It is reported that the undercooling increases with increase in rate of cooling and concentration of alloying elements [24]. The effect of cooling rate has also marked significant effect on the grain size, SDAS, morphology of Si particles and other iron based intermetallics and distribution of microstructural constituents. The increase in cooling rate refines grain size, reduce secondary dendrite arm spacings, modify the morphology of Si from elongated plate like morphology to fine fibrous or globular like morphology and decreases the size of intermetallics regardless of their type. The cooling rate refinement of the morphology of Si particle is described based on surface energy theory of interface of Al-Si particles [10]. The rate of growth of solid interface depends on the balance between latent heat of fusion released on solidification and heat flow rate across the solid-liquid interface. The latent heat of fusion for Al and Si is 396 J/g and 1411 J/g respectively. The thermal conductivities of Al and Si are 205 W/mK and 83 W/mK respectively in pure form. Due to large difference in their thermal conductivities and latent heat of fusion, Al will solidify faster than Si. Hence, growth of Al leads during eutectic solidification. As rate of cooling increases, growth of Al over Si increases and cause encasement of the entire Si particle which is lagging behind as shown in Fig. 2.

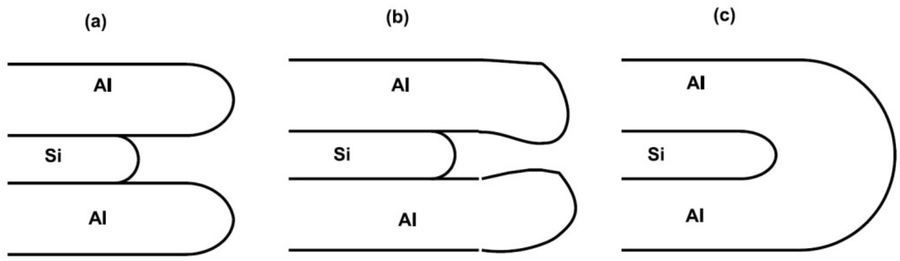

Figure 2. Eutectic solidification of unmodified Al-Si alloy

2.3 Solidification reactions

L. Backerud et al predicted that the following reactions would have occurred during solidification of Al-Si alloy [25].

Table 1. Solidification reactions at various temperatures

Sl.No.	Reaction	Temperature(K)
1	Development of Dendritic Network	888-883
2	a) L→ Al + Si b) L → Al + Al_5FeSi	883-835
3	a) L → Al + Si + Al_5FeSi b) L + Al_5FeSi → Al + Si + Al_8FeMg_3Si	837-831
4	L → Al + Mg_2Si + Si	831-822
5	L → Al + Si + Mg_2Si +$Al_8FeMg_3Si_6$	819-814

2.4 Grain refinement mechanisms

The grain refinement of a cast Al alloy component significantly influences its mechanical properties. Several studies have been done over years to discover various elements or combination of various elements to refine grains of Si based Al alloys, keeping in mind that the crystals with small lattice mismatch refine the grains as they favour heterogeneous nucleation sites for nucleation. P. Sritharan reported that Si based cast Al alloys can be refined by using Al-xTi-yB alloy with different Ti:B ratio [26]. Al-5Ti-1B is the most common master alloy that has been investigated and is widely used in industrial applications. GP Jones and C.D. Mayes et al observed that the ternary alloy, Al-Ti-B have $TiAl_3$ particles which dissolve in the melt and TiB_2 particles which act as heterogeneous nucleation sites [27,28].

P.S. Mohanty and J.E. Gruzleski reported that addition of master alloy like Al-Ti-B to the melt leads to formation of TiB_2, Al_3Ti, AlB_2, AlB_{12} particles [29]. Here titanium boride (TiB_2) particle act as heterogeneous nucleation sites for α-Al matrix when excess Ti is added by using master alloy like Al-5Ti-1B (Ti:B > 2.2:1) . P.S. Mohanty et al, J. Spittle and P. Schumacher identified that Ti in combination with Si forms Al-Ti-Si phase, at TiB_2/melt interface, which acts as heterogeneous site for nucleation of α-Al grains [29,30,31]. P.S. Mohanty et al observed that when an excess amount of Boron is added in the form of master alloy like Al-3Ti-3B, a layer rich in boron is formed at TiB_2/melt interface which lead to heterogeneous nucleation of α-Al phase [32]. Hence according to previous research, it can be concluded that the Ti:B ratio has a significant effect on refinement of grains. However, the optimum ratio between Ti and B is not mentioned clearly in any of the investigations yet.

Moreover, master alloys like Al-Ti-B have significant disadvantage. It has been reported that since Al_3Ti and TiB_2 particles have a density higher than the density of pure Al, this leads to segregation of particles which has the potential to nucleate α-Al grains and hence increase the melt holding time. Another disadvantage observed by R. Ghomachi is that the application of Ti as a grain refining agent would lead to the formation of flake like Al-Ti-Si phase which deteriorate the mechanical properties and casting properties of Si based Al alloys [33].

G. Sigworth et al and P.A. Tondel et al found that the master alloys with only B content are good grain refining agents in Si based Al alloys [34,35]. S. Nafisi et al reported that when boron is more than 200ppm, added in the form of master alloy like Al-4B, the supercooling effect of melt was eliminated and there was a significant increase in nucleation temperature relative to growth temperature which refined the grains effectively in Silicon based Aluminium alloy [36]. Y. Birol observed that Ti free samples treated with Al-3B master alloy result in fine grains of 200 µm diameter and are globular in shape [37]. It was found that Al-B alloys form AlB_2 and AlB_{12} particles in Al melt. However, Sigworth et al reported only AlB_2 particles are responsible for grain refinement whereas even at low Ti content, AlB_{12} particles get transformed into TiB_2 particles [38]. S. Nafisi et al found that these TiB_2 particle get enclosed inside AlB_2 and become heterogeneous site for nucleation of α-Al phase [36]. The quantity of B should be optimum so that there is no agglomerated B intermetallic on the microstructure. As compared to $TiAl_3$ and TiB_2 particles, AlB_2 has lowest density difference to pure Al and does not cause any poisoning effect with Si which make this phase unique to refine Ti free Al-Si alloys.

Sebastian F. Fisher et al remarked that Ti when combined with low B content of about 50ppm, highest eutectic supercooling is achieved and highest tensile strength is obtained. [39]. Whereas B content of about 150ppm in a titanium free Al-Si alloy like A356 alloy, smallest grain size is achieved and high elongation to fracture is obtained. Moreover, Lu Wang and Kang examined that B is powerful grain refiner than Ti [40].

On comparing the potential for nucleation of different crystals in Si based Al alloys, it is found that:

- $TiAl_3$ has poor nucleation potency and also highly soluble in Al melt. Hence a high amount of Ti is required to refine microstructure.
- TiB_2 particle has excellent nucleation potency and is hardly soluble in Al melt. Hence the refinement is long lasting.
- AlB_2 has the best potential for nucleation. However, AlB_2 readily dissolves in Al and also undergo reaction with Ti and Si in the melt. Hence undesirable sludge may form in the furnace when used for long intervals.

Sigworth and Guzowski developed a grain refiner that has a high potential for nucleation as that of AlB_2 and is insoluble in melt like TiB_2 particle [34]. The chemical formula for such a grain refiner is $(Al,Ti)B_2$ which was also termed as mixed boride.

It is believed that a small amount of Ti(0.02 wt.%) is required for Al-B master alloy addition but not necessary for TiB_2 type grain refiner like Al-xTi-yB addition. Also, it was reported that on adding 10-20ppm of B through master alloy addition like Al-5Ti-1B or Al-3Ti-1B results best grain refinement. This reduces the requirement of high content Ti. Low Ti content eliminate the tendency to form sludge in furnace.

It was detected that on adding Al-Ti-B based master alloy to the melt in such a way that Ti content is < 0.15 wt.%, the boron particles are found at the grain centres whereas Ti rich dendrites grow outside the grains. Some researchers found that Al-B particles are pushed toward the grain boundaries and $TiAl_3$ particles are at grain centres.

Sigworth and Backerud et al reported that $TiAl_3$ particles are best heterogeneous sites for nucleation of α-Al phase as compared to TiB_2 particle [41,42]. Davis et al, Maxwell and Hellowell identified the presence of $TiAl_3$ in α-Al matrix [43,44].

Recently Choongdo Lee examined that the optimum amount of Ti to be added should be in the range of 0.06 wt.%-0.15 wt.% to reduce micro-porosity, dendrite arm spacing (SDAS) and excellent grain refinement [45]. Moreover, there is an improvement in properties like tensile strength of the component on adding optimum Ti content. It was observed that excessive content of Ti reduces refinement of grains in case of A356 alloy and also deteriorate tensile properties to a range similar to that of an alloy without addition of Ti.

Y. Birol found that excess Ti in the form of Al-Ti-B based master alloy perform well in case of wrought alloys rather than foundry alloys [46]. Whereas excessive B content in Al-Ti-B or Al-B master alloys perform best for foundry alloys and depend on AlB_2 or $(Al,Ti)B_2$ particle for refinement of grains.

2.5 Modification mechanisms

In general, the master alloys that are used to refine grains of Si based Al alloys are Al-Ti, Al-Ti-C, Al-Ti-B, Al-Ti-C-Re (Re here is rare earth metals), etc. These master alloys are also termed as grain refiners. Moreover, the elements that are used to modify the shape of Si particles are Na, Sb, Sr and other rare earth metals like Lanthanides, Yb and Sc. One of the popular master alloy is Al-10Sr alloy which are also known as modifiers. They are added to the base metal to modify the needle/plate like morphology to fine fibrous form of Si particles to reduce stress concentration generated by Si particles in eutectic/ inter-dendritic regions of α-Al phase.

In Si based Al alloys, Si particles are having coarse and needle/acicular morphology which act as stress concentration sites and deteriorate mechanical properties of the alloy. Hence modification can be done by adding element like Na, Sr, Sb etc, in the form of master alloys.

It has been reported that Na undergoes fading effect faster whereas Sr has an incubation time and its effect is long lasting. W. Meyer observed that casting alloys modified with Na has fine micro-porosity distribution than that of Sr modified or unmodified alloys [47]. Antimony (Sb) can be used for permanent modification but is rarely used in foundry as it forms toxic compounds.

Couture reported that Sr addition with or without the presence of transition elements like Mn develops α phase inter-metallics which has Chinese script morphology [48]. This type of morphology reduces the formation of β phase needles. S.A. Kori et al found that about 0.02 wt.% of Sr can completely modify Al-7wt.% Si alloy within a holding time of 2 minutes [49]. Sergio Haro Rodriguez et al found that 0.04 wt.% and 0.06 wt.% Sr addition modified β phase needles to fine blocky shaped morphology [50]. Mondolfo et al and Lu SZ et al identified that about a few 100ppm of modifier addition changes Si particle from coarse plate like to fine fibrous like morphology and improve strength and ductility [51,52].

It is believed that there are two Si modification mechanisms

- **Surface energy theory**: On addition of chemical modifier, the surface energy of Al-Si solid interface decreases due to the increase in interface angle as shown in Fig. 3. This cause modification in eutectic structure by suppressing the growth of Si crystal

- **Interfacial poisoning theory**: As the Al-Si interface starts growing, the Impurity atoms like Na, Sr etc. deactivates or cause poisoning of the growth sites of Si particles [24]

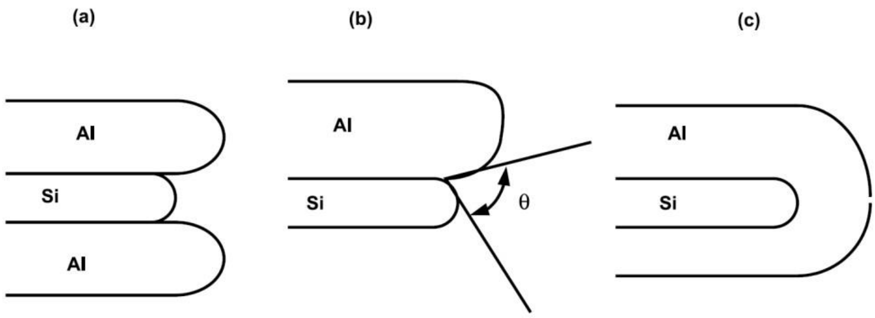

Figure 3. Eutectic solidification of modified Al-Si alloy

2.6 Poisoning effects

Improper addition of master alloys may cause negative effects on the mechanical properties of the alloy. S.A. Kori et al D. Qiu et al demonstrated that high Si content in Al-Si alloy on adding Al-Ti-B based master alloy cause poisoning effect due to reaction between Si and Ti which form Titanium Silicides like $TiSi_2$ and Ti_5Si_3 which has crystallographic mismatch with α-Al and can coat Al_3Ti particle and reduce its nucleation potency and hence reduce grain refinement of α-Al grains [53,54].

Liao and Sun et al observed when only B is used as grain refiner, it may react with Sr, which is added as a modifier, to form SrB_6 particles which settle down in the crucible thereby reduces the modification ability of Sr [55]. M. Timpel et al found that 200-300ppm of Sr is found to be optimum quantity for best results for modification of Si morphology[56]. Kazchiro Nogita et al examined that Sr:B ratio should be greater than 0.4 to retain Sr for modification of morphology of Si particles [57].

2.7 Heat treatment process

A controlled heat treatment processing of Al alloys can influence the mechanical properties significantly like strength, toughness, ductility, residual stresses, thermal stability, corrosion resistance, stress corrosion cracking resistance and dimensional stability. In general, heat treatment process include homogenisation, annealing and age hardening which involves solutionizing , quenching and then artificial/natural aging to obtain precipitates.

In order to improve toughness in the presence of cracks(fracture toughness) and yield strength, T6 type of heat treatment process is generally performed.

It is believed that the microstructure and alloying elements are also responsible for affecting the heat treatment efficiency of Si based Al alloys (hypoeutectic alloys) other than temperature and time.

A Si based Al alloy like A356 is a heat treatable alloy. On age hardening, the alloy is strengthened by precipitation of Mg_2Si particle and eutectic Si particle after T6 treatment. Various T6 heat treatment methods developed in China, USA and Japan in case of A356 alloys. But for effective energy consumption and minimum production efficiency, solution treatment process should be at a temperature of 540°C for more than 4hr aging should be at a temperature of 150°C for more than 6 hr.

Z. Ma et al found that there is an improvement in toughness due to modification of eutectic Si morphology and also due to dissolution and fragmentation of intermetallic when samples were treated by T6 heat treatment process [58,59]. S. Shivkumar et al examined the solution treatment effects on the characteristic of Si particle and also on the tensile properties of A356 alloy [60]. Wan Li et al studied that the eutectic microstructure of Al alloy of grade A390 can be refined and improvement in its properties can be obtained by optimised heat treatment process [61].

In T6 heat treatment process of Al-Si alloy there are two steps to be followed. One is the solutionising process and other is the artificial aging process.

- In solutionising process, α-Al becomes saturated with Mg and Si particles and cause spheroidization of Si near eutectic region.
- In artificial aging process, precipitation of strengthening phase, Mg_2Si is obtained.

Some researchers found that the solutionising temperature and size of Si particles affect the spheroidization time of Si particles.

Zhang D.L. eta al examined that a short solutionising period of about 30 minutes at a temperature of 540-550°C is sufficient to obtain similar mechanical properties as that of a solution treatment period of 6hr [62]. Yu Z. et al suggested that an optimum solutionising time of 2hr at 540°C from the calculation of thermal diffusion test [63]. Estey CM. et al and Rometsch P.A. et al observed that at maximum peak aging time of 2-4hr and a temperature of 170°C can improve the yield strength of A356 alloy to maximum [64,65].

2.8 Fretting wear

Nowadays, Al alloys are used in manufacturing of automobile parts like crankshafts, engine blocks, piston rings etc. as most of the machinery parts are subjected to cyclic/repeated motion or vibration of small amplitude in the range of microns under the application of applied load, there might be some loss in material which in turn cause loss in dimensional tolerances and deteriorate the contact surfaces. This type of wear or damage is termed as fretting wear. To analyse the life span of such components, it is important to study the fretting failure mechanism. Since fretting wear is one of the complicated wear phenomena, it has become a challenging area of research in recent era.

D.W, Hoeppner et al and M.H. Attia et al observed that fretting initiates crack faster and hence reduces fatigue life as compared to that observed due to conventional wear failure without fretting [66,67]. Fretting causes premature failure in many applications like bolted and riveted joints, dovetail contact area of blade root assembly in turbine blades of gas turbine engines, metallic ropes and cables, valve to valve seat assembly in IC Engines etc. Factors that influence fretting damage/fatigue are applied loading conditions, sliding amplitude, sliding frequency, sliding time, environmental conditions like ambient temperature, humidity, hardness of contact surfaces, surface conditions, coefficient of friction, tangential force/frictional force etc.

J.M. Dobromirski reported that among all the factors, frictional coefficient is one of the factors which influence fretting process significantly [68]. The mechanical interlock between the asperities of contacting surfaces and the adhesive bond decides the frictional coefficient parameter. This parameter directly influences the tangential shear force which is also termed as frictional force. K.J. Nixetal and T.A. Venkatesh et al reported that the normalised frictional force which is the ratio of frictional force to applied normal load is responsible for fretting wear crack initiation and growth [69-71]. GX Chen et al announced that fretting wear and sliding wear undergoing reciprocating motion can be distinguished by analysing how easily the wear debris can escape from the surface contact zone and the stroke line [72]. Y. Berthier et al found that fretting wear and sliding wear undergoing reciprocating motion can be differentiated by rate of volume wear [73].

Fretting wear is dominated by gross sliding slip condition where stick zone is absent across the entire contact region. During fretting wear, stick-slip condition take place at the interface of two mating surfaces due to absence of pure sliding motion. In fretting wear, the sliding amplitude is very low (in micron) and the normal load applied is sufficiently high to restrict the wear debris to flow away from the original site. The tangential shear force is believed to be generated at the interface of contacting surfaces due to either of oxide debris trapped in between the asperities.

Fretting wear process is described in a variety of mechanisms. Hurricks reported that fretting wear process can be divided into three stages [74]. Initially, the frictional coefficient is high for a first few thousand fretting wear cycles and major mechanisms involved are metal transfer across the interface and adhesion process. Metal to metal contact is predominant in this stage.

In the second stage, wear debris exposed to oxygen present in the surrounding atmosphere to form oxide debris. These oxide debris begin to accumulate in the interface of contacting surfaces, they act as abrasives and cause abrasive action.

After extensive fretting wear cycles, the coefficient of friction attains a steady state condition where abrasive action of oxide debris is decreased by formation of a compact bed of debris which acts a s a work hardened layer. At this stage, surface damage may be caused by fatigue.

Water house and Taylor observed that dislocation pile up may cause formation of delamination layer which in turn cause material removal in the form of plates in later stages of fretting wear cycles [75].

Iwabuchi examined that in fretting wear process there is two different effects of wear debris [76].

- Oxide layer formation is an advantage during the process of fretting wear
- Abrasive action is detrimental during initial stages of wear

These factors depend on magnitude of sliding amplitude and normal load applied.

2.9 Dry sliding wear

Dry sliding wear is another type of wear that can be observed in most of the industrial applications. In this type of wear, the contact surfaces of both the specimens undergo wear due to continuous sliding along the interface under the application of load and under dry conditions. Ball/ Pin on disk type apparatus is used for performing such experiments.

Both hypoeutectic and hypereutectic Si based Al alloys are being used in tribological components under dry and lubricated conditions for long period of time. Some researcher reported that higher Si content improves the wear resistant property of the alloy [77]. A series of non-commercial alloys were studied by varying the Si content ranging upto 20 wt% under pin on disc type sliding wear apparatus [78]. J. Clarke et al studied dry sliding wear using pin on disk type tribometer [79]. They observed that the wear resistance of Al-Si alloy improves with increase in Si content upto eutectic composition. They also found that higher Si content may cause wear of counter specimen even though it is made of steel. On further study they reported that the Si content does not have significant effect on wear rate of Al-Si alloy. There may be other factors for loss of material on applied load but the predominant cause of wear is the removal of work hardened layers from the wear track [80]. E.V. Dewhirst and G. Vandelli reported that the optimum Si content for wear resistance is hypereutectic Al-Si alloy [81,82]. K Okabayashi and M. Kawamoto found that Si content has no effect on wear until its composition exceeds 20 wt % [83,84]. B.N. Pramila Bai et al identified that wear rate increases with pressure and the coefficient of friction is insensitive to variation in pressure, Si content and sliding speed. They also observed that a Si content of 4-24 wt% significantly improves the wear property of Al-Si alloy [85]. K. Rajavizadeh et al observed that dry sliding wear of these alloys are dominated by oxidative type of wear [86,87]. R. Antoniou et al and B.N. Pramila bai et al reported that dry sliding wear is caused due to formation of an iron rich layer on the surface. Moreover, in as cast Al-Si alloys, the process of heat treatment and addition of Mg may alter the nature of the layer and hence also the wear properties of the alloy [88,89].

Further investigations were made in order to predict the effect of sliding speed on wear characteristics of the alloy. A.D. Sarkar found that with increase in sliding speed, wear rate increases resulting reduction in surface hardness [90]. K. Mohammed Jasim found that the wear rate decreases with increase in sliding speed in case of pure aluminium and its alloys [91]. S.K. Biswas et al and N. Saka et al reported that there were regions of increase and decrease in wear rate with steady increase in sliding speed [92,93]. It was observed that the mechanisms of wear at higher sliding speeds are different from that at lower sliding speeds. Some of the theories like the delamination theory could not explain wear characteristics at high sliding speeds [94]. Hence it is necessary to study the wear behaviour of the alloy by varying the sliding speeds. K. Mohammad Jasim et al reported that in Al-Si alloy, under the conditions of adhesive wear, wear rates decrease with increase in sliding speeds upto 150m/min. He also identified that the depth of damage of sub surface, size of wear debris and topography of worn surface are factors that indicate that the wear rate increases under oxidative conditions of wear with increase in sliding wear [95]. Subramanain also investigated the effect of sliding speed on wear rate of eutectic Si based Al alloys. He found that initially the wear rate decreases and then subsequent abrupt increase in wear rate with increase in sliding speed [96].

Chapter 3

Research approach

3.1 Purpose and aim

Si based Al alloys are increasingly found to be attractive for automotive applications. The challenge is to improve the mechanical properties of these alloys by microstructural engineering. The alloying elements mark significant contribution to the mechanical properties like strength, ductility, toughness, hardness and wear resistance. Mechanical modification by squeeze casting and chemical modification by suitable grain refiners and eutectic Si modifiers is one of the most promising ways to improve the mechanical properties of these alloys. The aim of this research work is to understand the effect of squeeze casting and grain refinement and modification on several microstructural characteristics such as SDAS, Si particle morphology and intermetallic phases. The effect of heat treatment on microstructure is also studied. Finally, wear properties of these alloys under fretting wear and dry sliding wear are also analysed.

3.2 Research design

The present research work focuses on some of the real industrial issues concerning the casting process of Al-Si alloys such as the amount of alloying additions i.e. master alloy additions like grain refiners and grain modifiers, which influence the performance of these alloys. Efforts have been made to investigate the potential for improving wear properties of the alloy. The effect of heat treatment on microstructure was also investigated. Prior to each phase of research, a comprehensive literature survey on selected topics was done to collect relevant data and information in relevant research works. As per the literature survey, it was reported that the Ti:B ratio should be greater than 2.2:1 for improving the mechanical properties of the alloy and hence Al-5Ti-1B was chosen as a grain refiner in which the ratio of Ti and B is 5:1 i.e about 750ppm of Ti and 150ppm of B were obtained in the final castings.

Moreover, from previous research work, it was observed that about 0.02 wt% Sr (i.e about 200ppm of Sr) can modify the morphology of Si particles effectively [49] and also to reduce the poisoning effect of Sr and B, the ratio must be greater than 0.4 [57]. Hence, an optimum amount of Sr was added in the form Al-10Sr which acts as a grain modifier so that the modification ability of Sr is enhanced and the ratio between Sr and B is maintained in the final castings i.e. about 200ppm and 300ppm of Sr were obtained in the final cast product. Therefore, the ratio of Sr and B is 1.33 and 2 for A356+Al-5Ti-1B+Al-10Sr(200ppm Sr) alloy and A356+Al-5Ti-1B+Al-10Sr (300ppm Sr) alloy respectively.

Literature survey helped us to understand the lack of knowledge on this field of research and also helped in identifying the challenges and problems, the manufacturing industries are facing these days. Prior to framing of experimental plans, the reliability of the experimental set up was evaluated. Then the routine of experiments were designed and performed. The results were collected, analysed, evaluated and compared with the data obtained from the literature. The conclusions were made based on the data obtained and the results reported by previous research works. The flowchart of the current research approach is shown in Fig. 4.

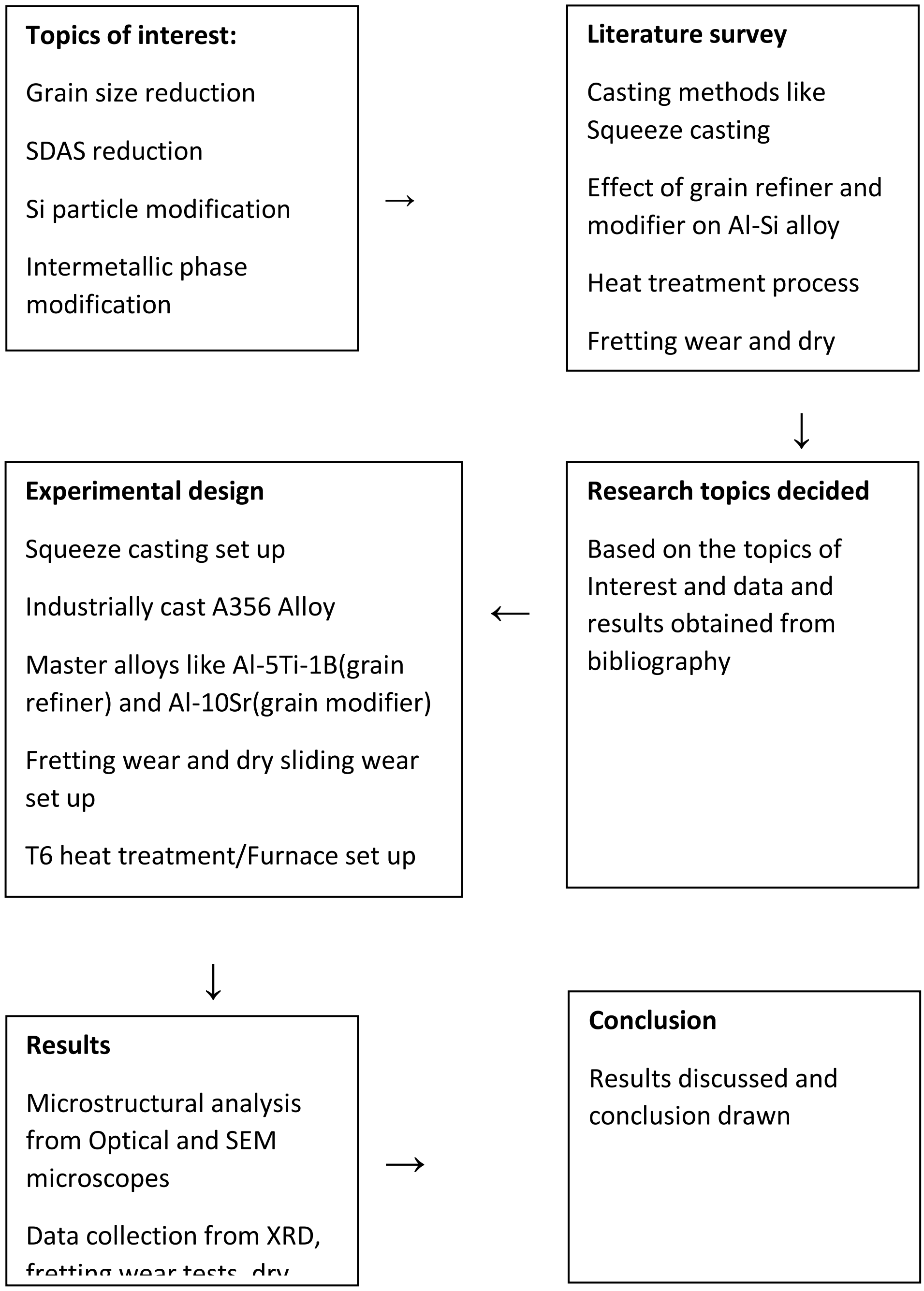

Figure 4. Flow chart of the research approach of current research work

The current research work comprises of four major topics:

1. Investigation of the effect of squeeze casting on microstructure of A356 alloy such as SDAS, grain size, morphology of Si particle and other intermetallic phases.
2. Investigation of the effect of grain refiner like Al-5Ti-1B and grain modifier like Al-10Sr on microstructural characteristics of A356 alloy.
3. Effect of heat treatment process on microstructural characteristics of A356 alloy.
4. Effect of squeeze casting, grain refinement and modification, T6 heat treatment on wear properties of A356 alloy like fretting wear and dry sliding wear.

Chapter 4

Experimental work

Experimental work in this research first consisted of squeeze casting of Al-Si alloy A356 with and without grain refiner Al-Ti-B and Sr modifier. The effect of squeeze casting and chemical modification by grain refiner and modifier addition was subsequently studied with microstructure analysis. The effect of heat treatment on different alloys was also investigated. Finally, the effect of microstructural refinement on wear properties during fretting wear and dry sliding wear was analysed.

4.1 Raw material and its compositions

The composition of Al-Si alloy of grade A356/LM25 which is used for pressure-assisted/squeeze casting is given in Table 2. The other alloying elements like Ti, B and Sr are added by using master alloys like Al-5Ti-1B and Al-10Sr which would act as a grain refiner and a grain modifier respectively. The exact composition of the master alloys are shown in Table 2.

Table 2. Alloy composition in wt.%

Alloy	Si	Mg	Ti	Fe	Sr	Cu	B	Ca	Others	Al
A356	7.04	0.3783	0.1346	0.09	0.0154	0.0005	-	-	0.051	Balance
Al-5Ti-1B	-	-	5.21	-	-	-	0.97	-	<5	Balance
Al-10Sr	0.2	-	-	0.3	9-11	-	-	0.03	0.15	Balance

4.2. Casting of Al-Si alloys

Fig. 5a. shows the setup of SWAM EQUIP Bottom pouring type stir casting machine with squeeze casting assembly which was used for casting the alloy samples studied in this work.. The dimensions of the squeeze casting die cavity are 300mm height and 50mm diameter. Hence keeping in view the dimensions of the cavity, suitable amounts of the raw materials were prepared. For this purpose small sized (40x40x40 mm) blocks were cut from the (70x70x750 mm) ingot supplied by Hero MotoCorp Ltd. as shown in Fig. 5 b. Considering the density to be 2.6g/cm^3, raw material of 1500g was prepared for casting.

(a) (b)

Figure 5. Raw material and machine used for casting (a) Squeeze casting machine (b) Industrially cast as-received A356 alloy ingot

The temperature of the furnace was set at 850°C and temperature of the crucible/melt was set at 800°C. The small sized blocks of raw materials were inserted into the furnace once the required temperature was attained. The master alloys to be added to the melt, were preheated prior to casting to remove any moisture content present. To maintain a controlled atmosphere inside the furnace and to prevent contamination of unwanted gases which may lead to gas defects, degassing was done by supplying inert gas like argon periodically at a flow rate of 2 LPM.

When the raw material was completely melted, the stirrer was operated continuously at a speed of 300rpm for 15-20 minutes so that all the alloying elements are distributed in uniform manner in the entire volume of liquid metal.

To obtain a surface finish of higher quality of the cast product, graphite coating was done on the metal surfaces where the molten metal comes in contact during casting operation. Surfaces like inner diameter of mould cavity, runner, thermocouple and crucible were coated prior to casting.

The mould cavity and runner was also preheated to 200°C and 750°C respectively. The runner is preheated so that the molten metal does not get solidified during the flow of liquid metal through it. The mould cavity is preheated to prevent the damage of the die due to thermal shock/stresses caused by large thermal gradient.

The casting machine set up was equipped with a SCF process monitoring system which readily measures the temperature of the heating systems, control stirrer speed, adjusts bottom pour valve, monitor inert gas supply rate for degassing and control squeeze pressure.

The liquid metal was finally poured into the mould cavity via the runway. A hydraulic pump of 40T capacity was used to control the motion of the piston into the die cavity to pressurise the metal during solidification. A pressure of 40 tonnes (about 200MPa) was applied for all the castings. After solidification of liquid metal, the piston is lifted and the two halves/end plates of the die are removed to obtain the solidified product as shown in Fig. 6. The castings that were prepared are:

- A356 alloy
- A356 alloy+ Al-5Ti-1B (750ppm Ti and 150ppm B)

- A356 alloy+ Al-5Ti-1B(750ppm Ti and 150ppm B)+Al-10Sr (200ppm Sr)
- A356 alloy+ Al-5Ti-1B(750ppm Ti and 150ppm B)+Al-10Sr (300ppm Sr)

The calculations made for adding alloying elements are as follows:

- Density of A356 alloy: 2.67 g/cm^3
- Volume of the mould cavity i.e. volume of the product:
  V= $\frac{\pi}{4} \times D^2 \times L$ = $\frac{\pi}{4} \times 5^2 \times 30$ = 589.048 cm^3
- Mass of the cast product to be obtained = 1572.758g ≈1600g

Addition of master alloys were done by calculations using Unitary Method:

1. To produce an alloy of A356 + Al-5Ti-1B (750ppm Ti, 150ppm B), the following calculations were made.

If 5 wt % of Ti present in 1600g of master alloy (Al-5Ti-1B)

Then, in order to obtain 0.075 wt % Ti (750ppm) in the final cast product, the amount of master alloy to be added is = $\frac{1600}{5} \times 0.075$ = 24g of Al-5Ti-1B alloy

Therefore, the amount of A356 alloy to be added is = $1600-24 = 1576$g

2. To produce an alloy of A356 + Al-5Ti-1B + Al-10Sr (750ppm Ti, 150ppm B, 200ppm Sr), the following calculations were made.

If 10 wt % of Sr present in 1600g of master alloy (Al-10Sr)

Then, in order to obtain 0.02 wt % Sr (200ppm) in the final cast product, the amount of master alloy to be added is = $\frac{1600}{10} \times 0.02 = 3.2$g of Al-10Sr

Amount of Al-5Ti-1B to be added is 24g (as calculated earlier)

Therefore, amount of A356 alloy to be added is =1600-(24+3.2) = 1572.8g

Similar calculations were made for adding alloying elements to the cast product.

All the samples used for investigation were extracted from the lower end of the cast cylindrical products at a section 20-30mm from the bottom.

Figure 6. Squeeze cast product

4.3 Sample preparation and analysis

For both optical microscopy and SEM analysis, the samples were cut using a wire EDM or an abrasive cutting machine and then polished using emery paper of various grades and finally polished using diamond paste for obtaining mirror finish to get rid of any scratches in the surface.

The polished samples were further etched by Keller's reagent, prepared by mixing 2ml of HF, 3ml of HCl, 5ml of HNO_3 and 190 ml of distilled water. The samples were etched for 20 seconds in order to reveal the various phases, grains and grain boundaries in the microstructure.

The optical image analysis was done using ZEISS Axio Inverted Microscope having a wide range of advance contrast methods. SEM image analysis was done using JEOL JSM-7610Plus Schottky Field Emission Scanning Electron Microscope equipped with EDS and EBSD.

4.4 Heat treatment

Small amples of dimensions (10x10x5 mm) extracted from squeeze cast samples were subjected to a T6 heat treatment process. A muffle furnace equipped with PID controller (programmable temperature controller) was used to control solutionising and aging temperature during T6 heat treatment process.The solution treatment was carried out at 520°C(below eutectic temperature i.e. 577°C to avoid localised melting) for 4 hours followed by quenching in the water immediately to room temperature and then artificial aging at 170°C for 2 hours followed by air cooling. The heat treatment cycle is represented in Fig. 7. The microstructures of heat treated samples was then observed under an optical microscope.

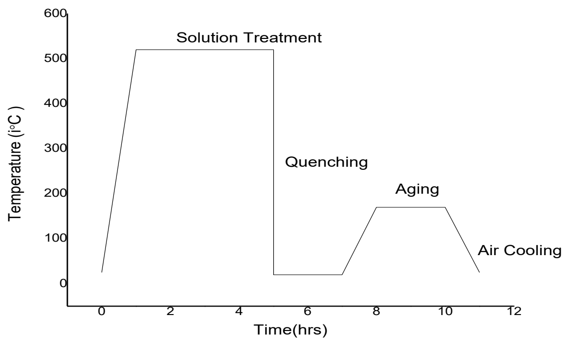

Figure 7. T6 Heat treatment process cycle

4.5 Fretting Wear

Fretting wear tests were conducted on as-received samples, squeeze cast A356 alloy samples and samples alloyed with grain refining agent and modifying agent. The tests were carried out using a DUCOM Linear Reciprocating Tribometer (Fig. 8), both at room temperature and at an elevated temperature of 100°C. Tribometer is equipped with a computer-controlled process monitoring system and a data acquition software, WINDUCOM 2010 which monitors the stroke or sliding amplitude, frequency, temperature, humidity, normal load applied, test duration and dwell time. It also measures the variation in coefficient of friction and frictional force with the number of fretting wear cycles during its operation. The load was applied on the counter specimen (also known as a upper specimen) by a lever connected to a dead weight through a string. The dimension of lower specimen used was (20x20x5 mm). A 15mm height and 6 mm dia. cylindrical pin made of high C steel ball of grade EN31 (hardness of 63 HRC) was used as the counter specimen. The tests were performed at a sliding amplitude of 250μm and a frequency of 10 Hz. The applied normal load were 5N, 10N, 15N and 20N. The time set for fretting wear contact was of 15 minutes.

(a) (b)

Figure 8. Fretting wear set up (a) Φ6 Steel pin in contact with test sample (b)String connected to dead weight where load can be varied.

4.6 Dry Sliding Wear

Dry sliding wear tests were performed on as-received and squeeze cast A356 alloy samples. The samples were tested using a DUCOM ball/pin on disk type tribometer as shown in Fig. 9. The machine has the provision to monitor coefficient of friction (COF) and wear depth of the specimen. A sliding amplitude of 0.15m/s and 0.25 m/s, sliding distance of 300m, load of 5N and wear track diameter of 10mm and 20mm were used as the parameters for the testing. A hardened steel ball of 8mm diameter was used as counter specimen while the test sample was made up of 50mm diameter and 5mm thickness disc. During testing the sliding takes place between the ball and rotating disc.

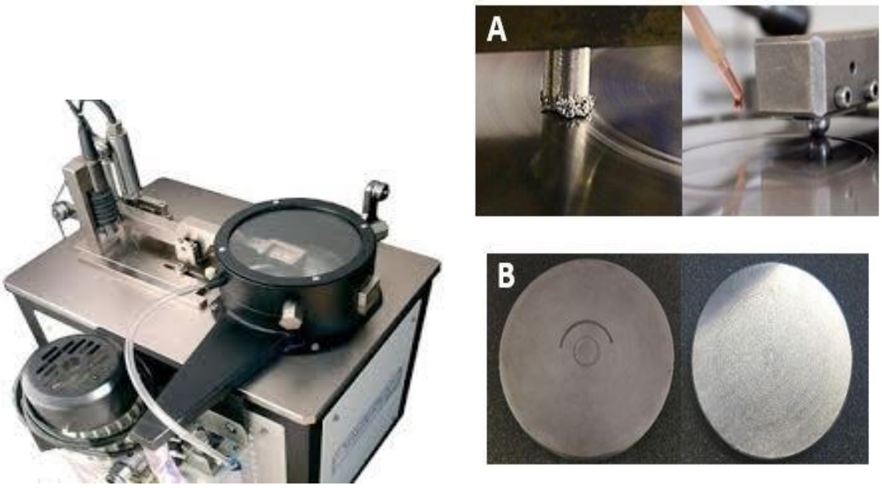

(a) (b)

Figure 9. Dry sliding wear test set up (a)Pin/Ball on disk tribometer (b) Test sample undergoing wear

Chapter 5

Results and discussions

5.1 Microstructural analysis using optical microscopy

5.1.1 Effect of squeeze casting on as-received A356 alloy

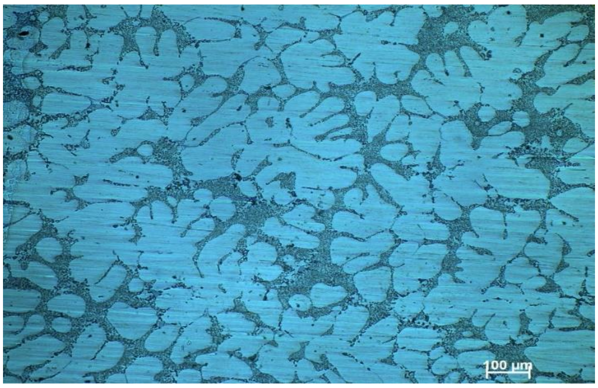

Figure 10. Optical image at 10X magnification of as-received A356 alloy sample

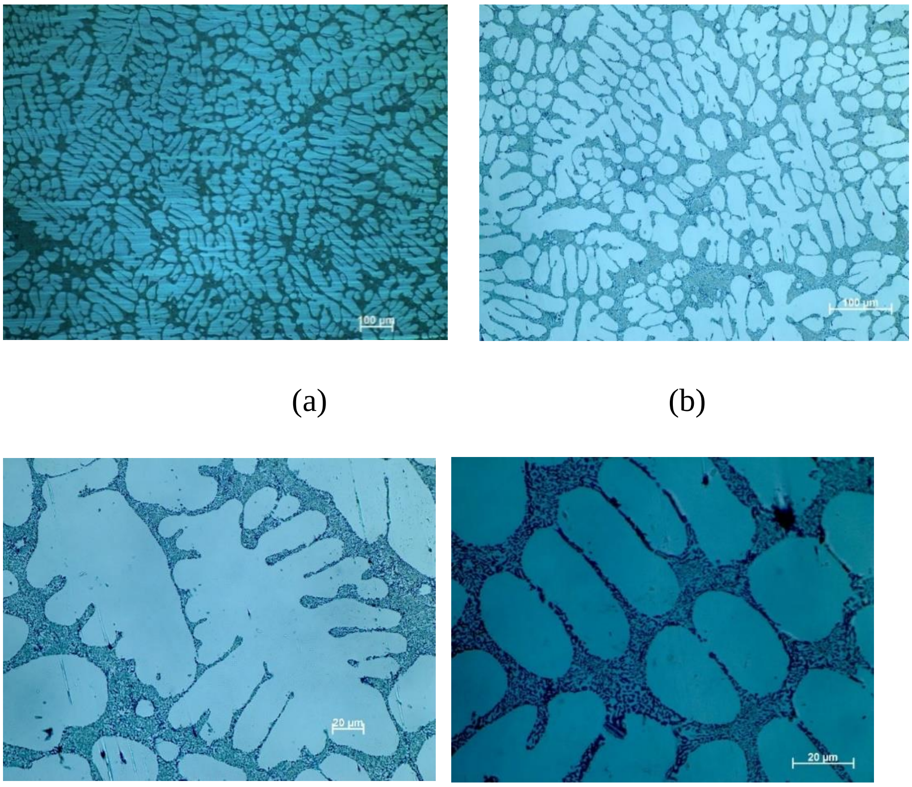

(a) (b)

(c) (d)

Figure 11. Optical images of squeeze cast A356 alloy samples at (a)10X (b)20X (c)50X (d)100X magnification

The following predictions may be made from optical image analysis:

- The volume fraction of the primary α-Al phase increases.
- The size of primary α-Al dendrites decreases (Figs 10 and 11a).
- The volume fraction of the eutectic phase decreases.
- Refinement of Si in the eutectic region is observed.
- The average SDAS (Secondary Dendrite Arm Spacing) was reduced from 45(+/-2) μm to 26(+/-2) μm (50% reduction)

Previously, similar predictions were made by M.T, Abou El Khair in case of squeeze cast Al-6Si0.3Mg alloy [97]

5.1.2 Effect of T6 heat treatment on as-received A356 Alloy

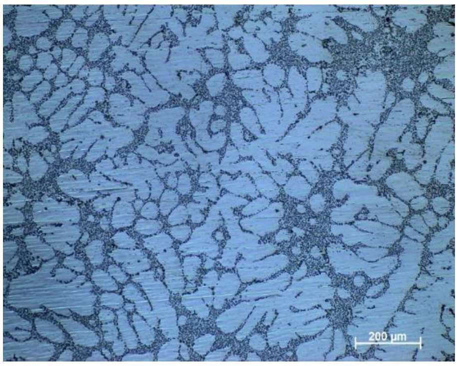

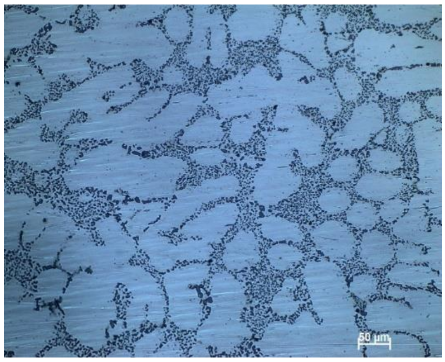

(a) (b)

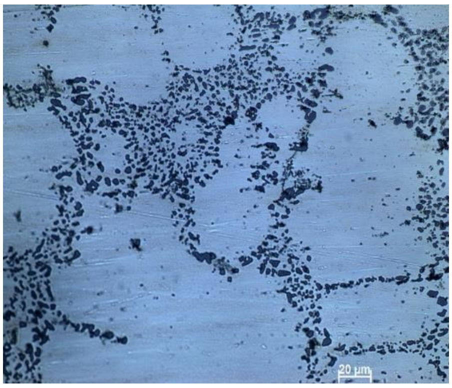

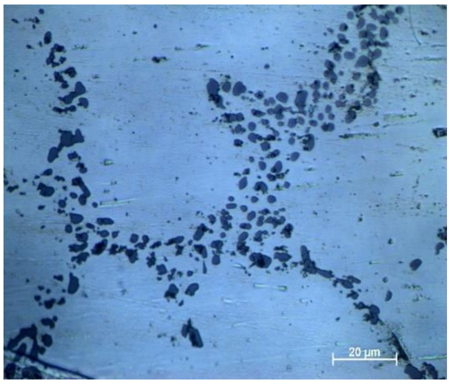

(c) (d)

Figure 12. Optical images of heat treated as-received A356 alloy samples at (a)10X (b)20X (c)50X (d) 100X magnification

5.1.3 Effect of T6 heat treatment on squeeze cast A356 alloy

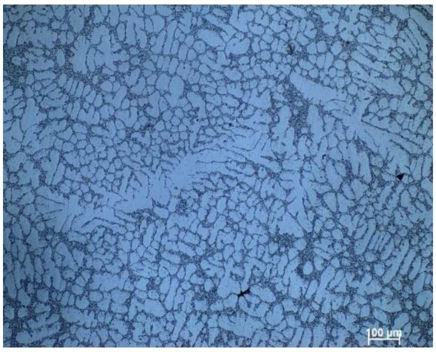

(a)

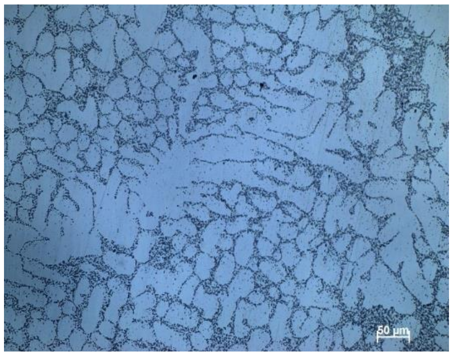

(b)

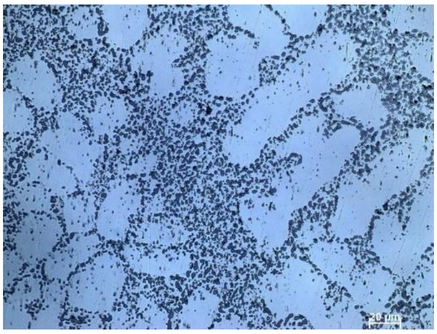

(c)

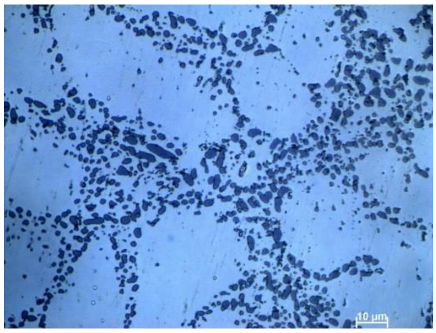

(d)

Figure 13. Optical images of heat treated squeeze cast A356 alloy samples at (a)10X (b)20X (c)50X (d) 100X magnification

T6 heat treatment was found to be more effective in case of squeeze cast specimens due to uniform precipitation (Figs. 12 and 13). After heat treatment, precipitation of intermetallics including Mg_2Si particles in interdendritic regions is found to be more dense accompanied with change in the morphology of Si particles.

5.1.4 Effect of grain refiner Al-Ti-B on squeeze cast A356 alloy

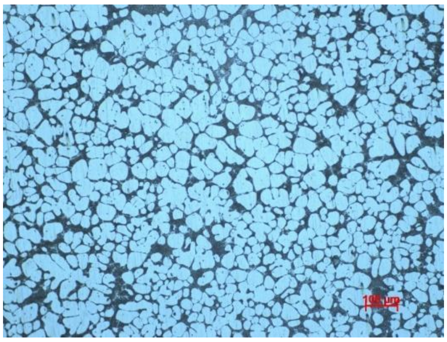

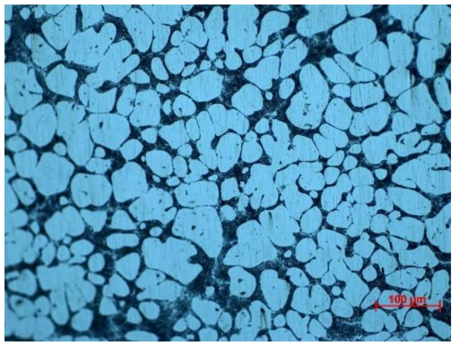

(a) (b)

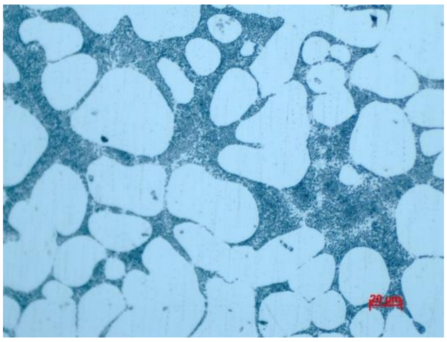

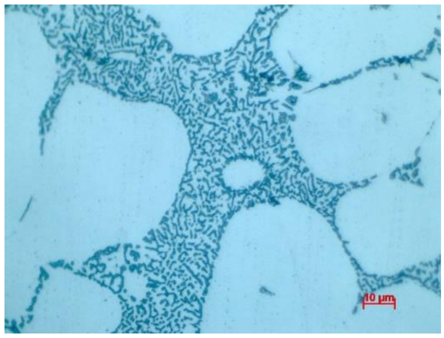

(c) (d)

Figure 14. Optical images of grain refined alloy samples using Al-5Ti-1B at (a)10X (b)20X (c)50X (d)100X magnification (750ppm Ti,150ppm B)

5.1.5 Combined effect of grain refiner Al-Ti-B and modifier (200ppm Sr) on squeeze cast A356 alloy

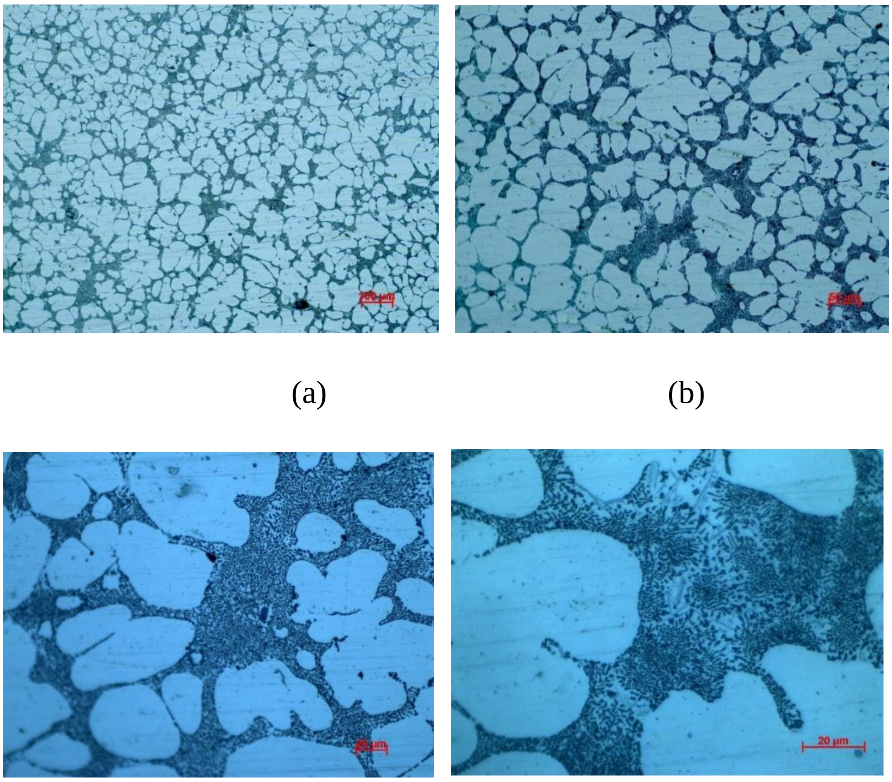

(a) (b)

(c) (d)

Figure 15. Optical images of grain refined and modified alloy samples using Al-5Ti-1B and Al-10Sr at (a)10X (b)20X (c)50X (d)100X magnification (750ppm Ti,150ppm B and 200ppm Sr)

5.1.6 Combined effect of grain refiner Al-Ti-B and modifier(300ppm Sr) on squeeze cast A356 alloy

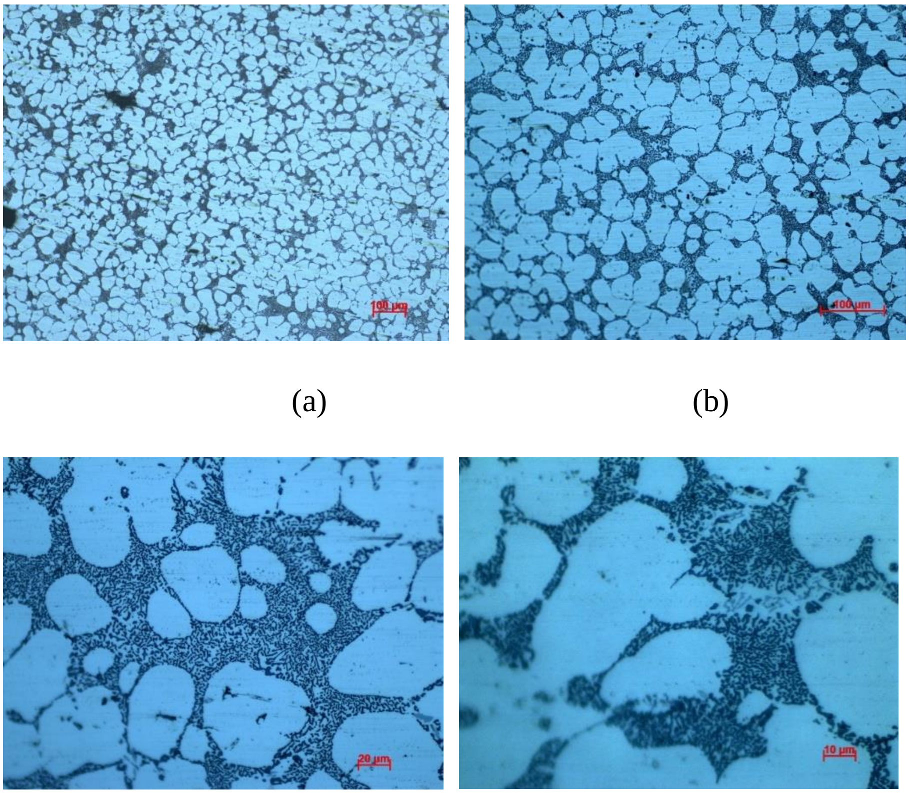

(a) (b)

(c) (d)

Figure 16. Optical images of grain refined and modified alloy samples using Al-5Ti-1B and Al-10Sr at (a)10X (b)20X (c)50X (d)100X magnification (750ppm Ti,150ppm B and 300ppm Sr)

The following observations are made after addition of grain refiner and modifier to the alloy:

- The average SDAS calculated for A356+Al5Ti-1B+Al-10Sr(200ppm Sr) was 20(+/-3) µm and that for A356+Al-5Ti-1B +Al-10Sr (300ppm Sr) was 20(+/-2) µm. There is not much change in SDAS with change in Sr content as Sr is responsible for changing the morphology of Si particles and Fe based intermetallics. It is the Al-5Ti-1B alloy which is responsible for refining the alloy from squeeze cast A356 alloy having SDAS of 26(+/-2) µm to squeeze cast A356+ Al-5Ti-1B having SDAS of 20(+/-3) µm

- Change in the shape of α-Al phase from tree like dendritic to globular shape (Figs. 11 and 14)
- Addition of Sr produces α-phase Fe based intermetallics which have Chinese Script morphology and also change in the shape of Si particles was observed (Fig. 16d).

5.1.7 Combined effect of T6 heat treatment and grain refinement on squeeze cast A356 alloy

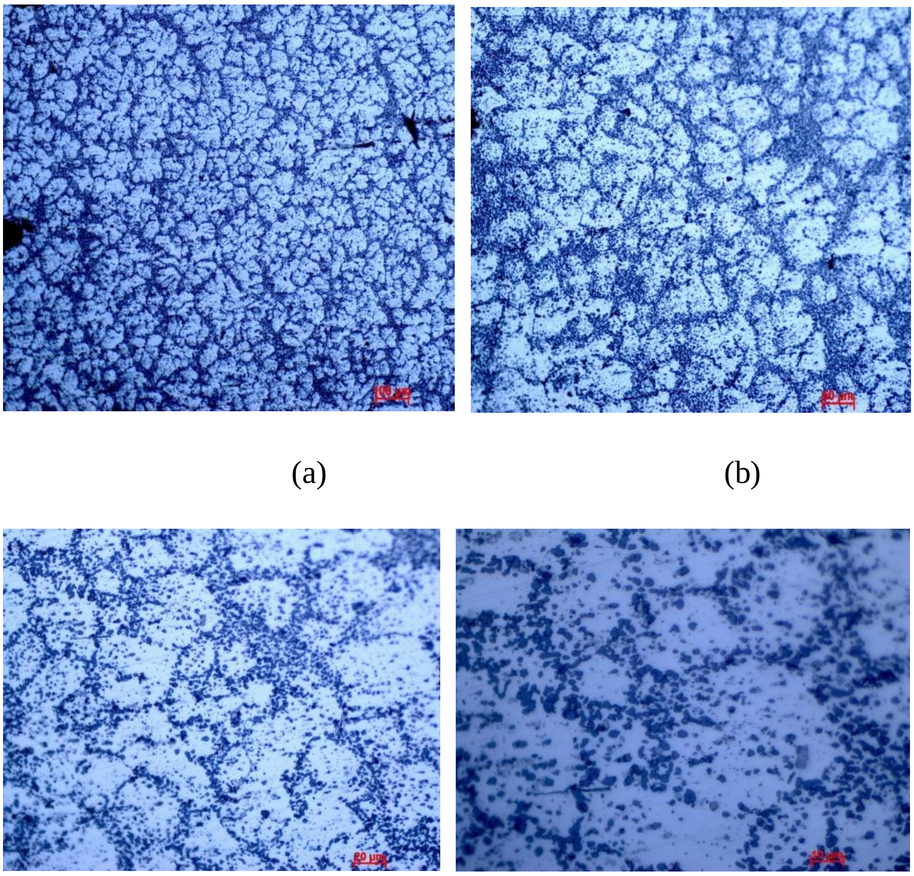

(a) (b)

(c) (d)

Figure 17. Optical images of heat treated and grain refined alloy samples using Al-5Ti-1B at (a)10X (b)20X (c)50X (d)100X magnification (750ppm Ti,150ppm B)

5.1.8 Combined effect of T6 heat treatment, grain refiner Al-Ti-B and modifier (200ppm Sr) on squeeze cast A356 alloy

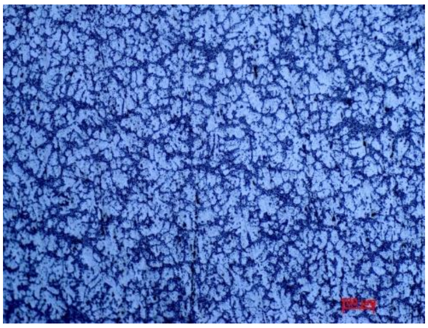
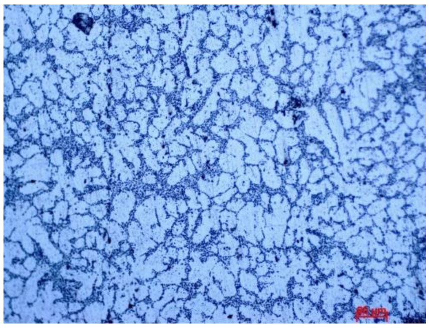

(a) (b)

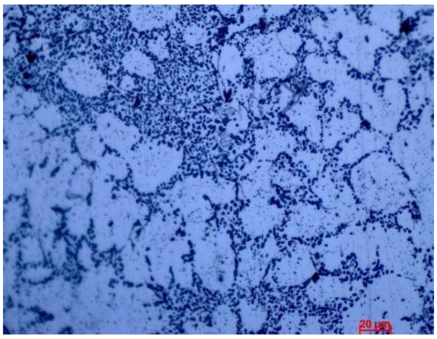
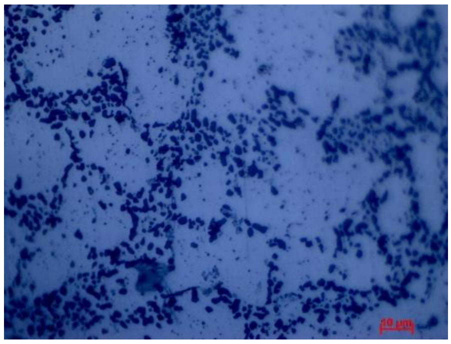

(c) (d)

Figure 18. Optical images of heat treated,grain refined and modified alloy samples using Al-5Ti-1B and Al-10Sr at (a)10X (b)20X (c)50X (d)100X magnification (750ppm Ti,150ppm B and 200ppm Sr)

5.1.9 Combined effect of T6 heat treatment, grain refiner Al-Ti-B and modifier (300ppm Sr) on squeeze cast A356 alloy

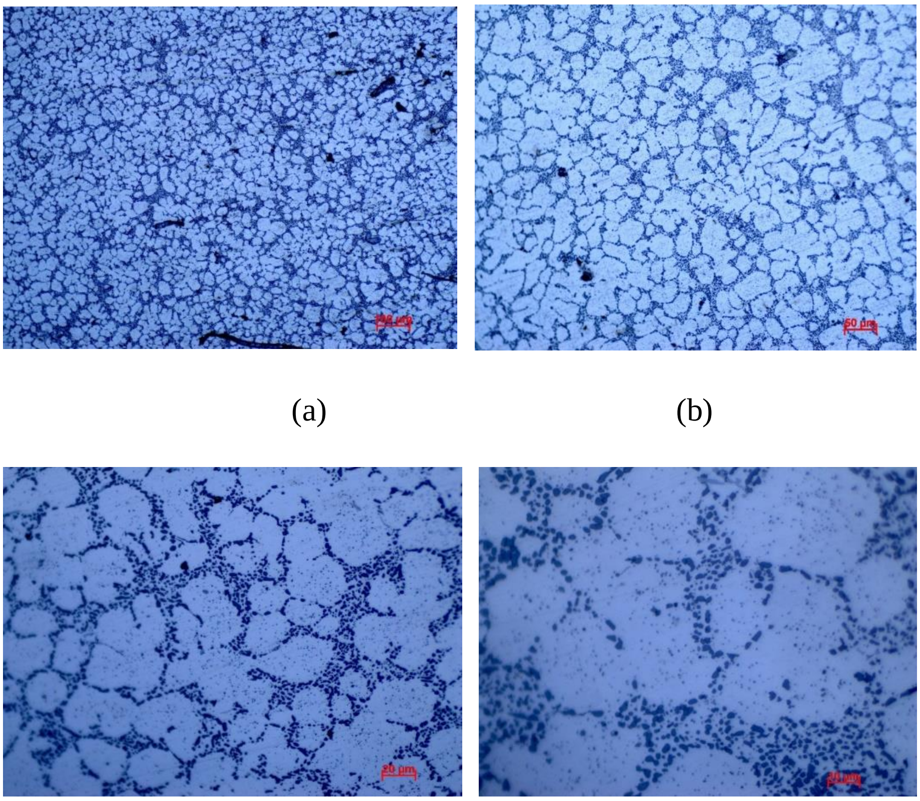

(a) (b)

(c) (d)

Figure 19. Optical images of heat treated,grain refined and modified alloy samples using Al-5Ti-1B and Al-10Sr at (a)10X (b)20X (c)50X (d)100X magnification (750ppm Ti,150ppm B and 300ppm Sr)

The following observations are made after heat treatment of grain refined and modified squeeze cast A356 alloy:

- Heat treatment was observed to be fruitful in case of grain refined sample as precipitation was observed to be uniformly distributed within the matrix of α-Al phase and also at the interdendritic regions of α-Al matrix (Fig. 17).
- Precipitation was not effective at higher Sr content. Sr modified samples show reduced precipitation within α-Al matrix than those without modifier addition. The interdendritic phases are also more refined with fine precipitation on addition of modifier

at 200 and 300 ppm when compared to samples without any modifier addition. (Figs.18 and 19)

5.2 Microstructure analysis using SEM

5.2.1 Effect of squeeze casting on as-received A356 alloy

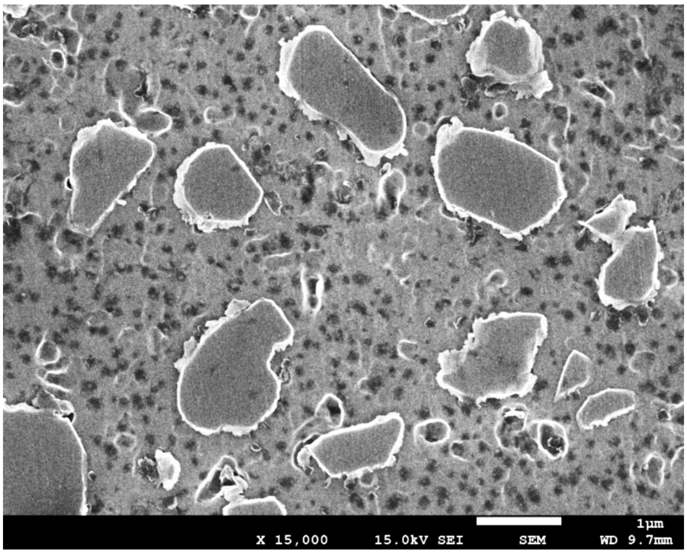

Figure 20. SEM image of as-received A356 alloy sample

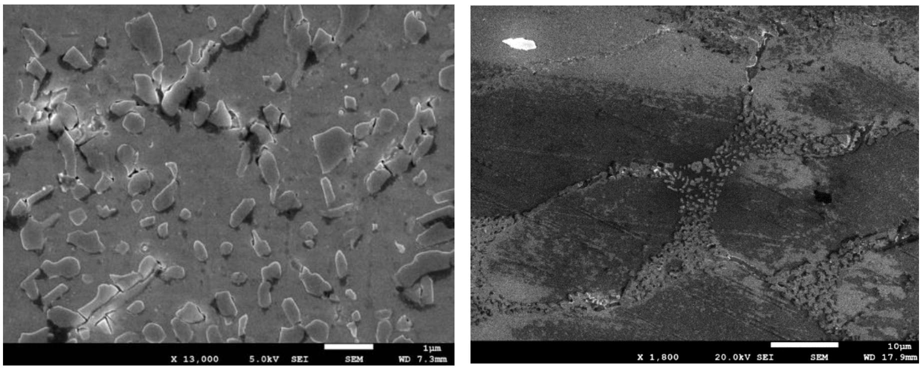

(a) (b)

Figure 21. SEM images of squeeze cast A356 alloy samples (a) Al-Si eutectic region (b) α-Al and eutectic Si phase

Reduction in porosity and change in the shape of Si particles was observed in squeeze cast samples (Figs. 20 and 21). Elongated Si particles were found to be broken into small fragments.

5.2.2 Effect of heat treatment on squeeze cast A356 alloy

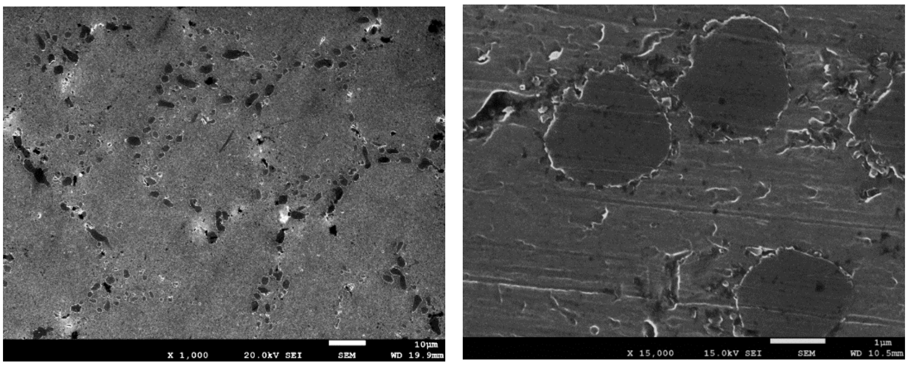

(a) (b)

Figure 22. SEM images of heat treated squeeze cast A356 alloy samples (a) Precipitation of Fe intermetallics (brighter regions) in eutectic zone (b)Spheroidal Si particles

Change in the morphological aspects of Si particles in the eutectic region from needle shape morphology to spheroidal shape morphology are observed after T6 heat treatment process (Fig. 22b).

5.2.3 Effect of grain refiner Al-Ti-B on squeeze cast A356 alloy

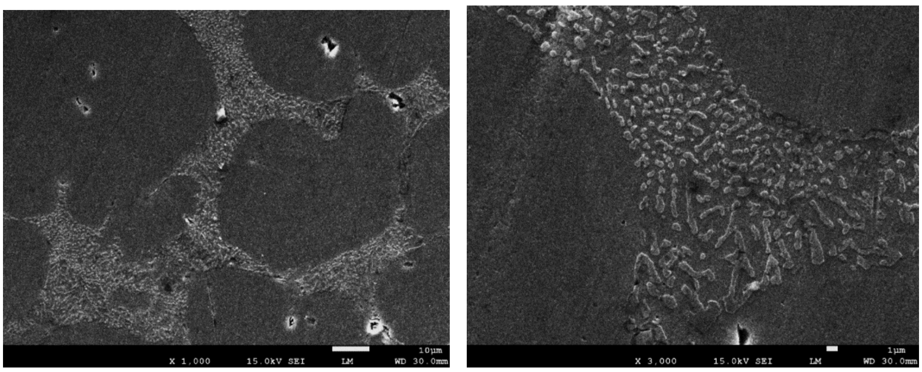

(a) (b)

Figure 23. SEM images of grain refined alloy samples using Al-5Ti-1B (a)α-Al and Si eutectic phase (b) unmodified Si particles in eutectic zone (750ppm Ti,150ppm B)

5.2.4 Effect of grain refiner Al-Ti-B and modifier Al-10Sr(300ppm Sr) on squeeze cast A356 alloy

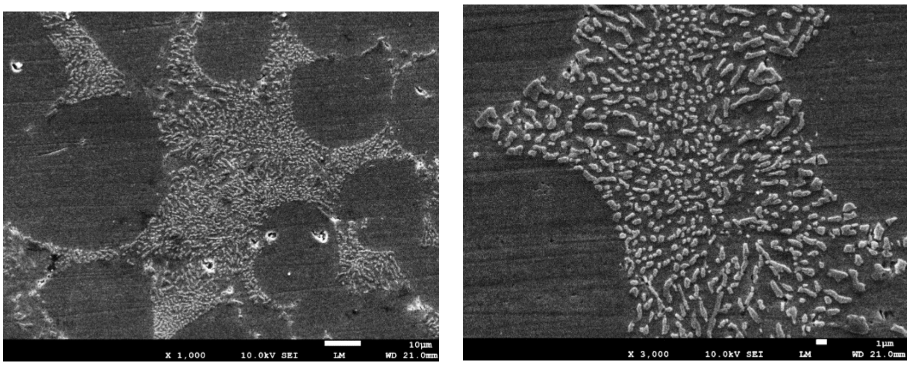

(a) **(b)**

Figure 24. SEM images of grain refined alloy samples using Al-5Ti-1B (a)α-Al and Si eutectic phase (b) partially modified Si particles in eutectic zone (750ppm Ti,150ppm B,300ppm Sr)

Presence of lamellar Si particles indicate that only partial modification occurred on adding Sr as a modifying agent (Fig. 24b). The morphology of α-Al matrix was observed to be more globular instead of dendritic after addition of grain refiner and grain modifier to the alloy.

5.3 Some of the major observations made from Optical and SEM analysis

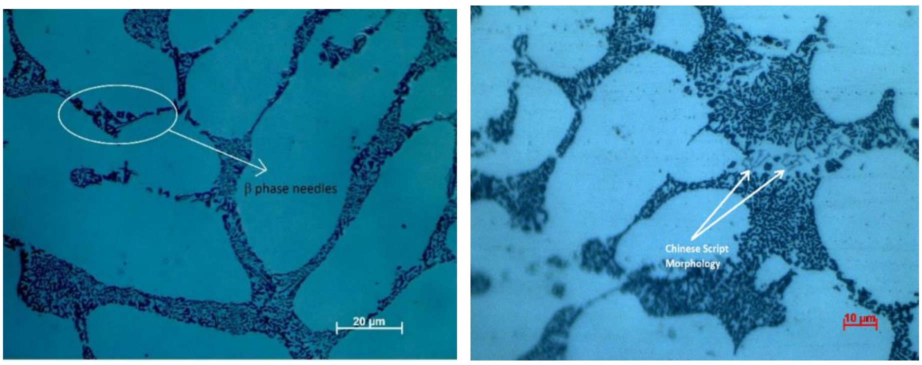

(a) (b)

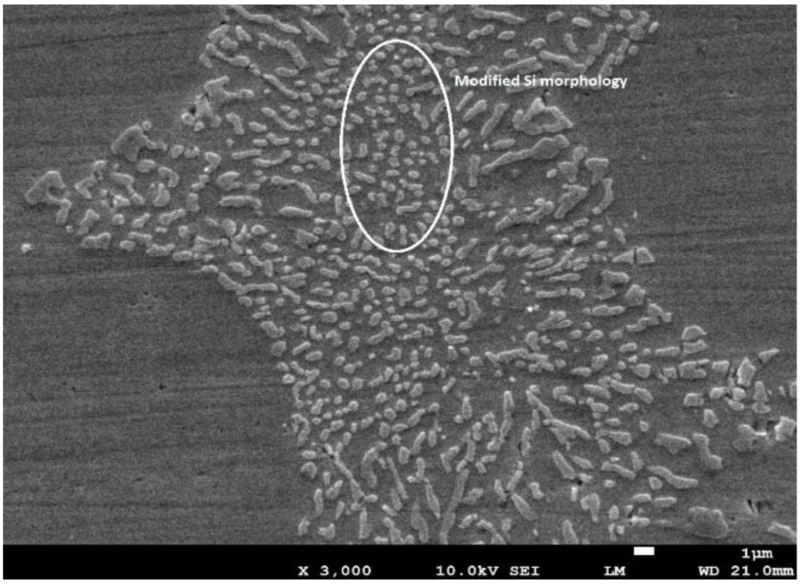

(c)

Figure 25. Microstructural images of A356 alloy samples (a) Optical image of unmodified A356alloy showing presence of Fe based β-phase needles (b)Optical image of Sr modified alloy showing Fe based α-phase intermetallic with Chinese script morphology (c) SEM image showing partial modification of Si particles

Some important observations made from Optical and SEM analysis are:

- On adding Al-5Ti-1B to A356 alloy, uniform distribution of eutectic phase was observed rather than concentrated over a small area as compared to non-refined alloy. Moreover, this was accompanied with reduction in SDAS
- Sr addition brought changes in the morphology of Si particles from needle/acicular shape to fine fibrous/spheroidal shape
- Sr addition developed α-phase intermetallic having Chinese Script morphology (Fig. 25b) and reduced formation of β-phase (iron rich intermetallic) needles thus reducing stress concentration sites.
- Presence of lamellar Si particles in some regions of the alloy depicted that only partial modification of Si particle was possible on adding Sr which may be due to reaction between Sr and B or may be due to insufficient Sr content (Fig. 25c). This was observed in both the cases where Sr content was 200ppm and 300ppm.

5.4 SEM analysis using BSE imaging

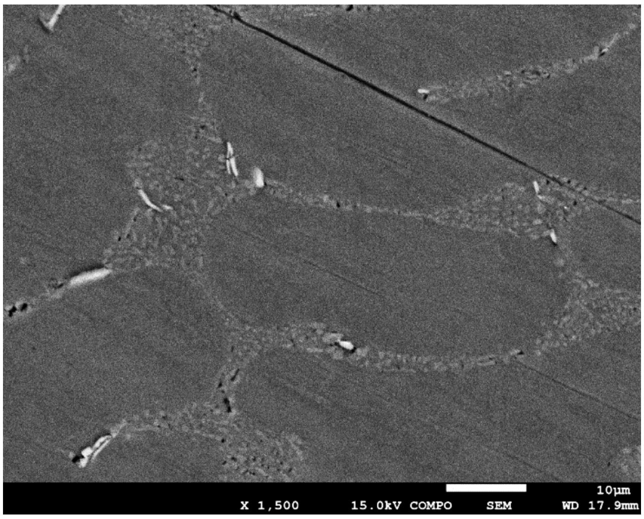

Figure 26. BSE image of squeeze cast A356 alloy sample

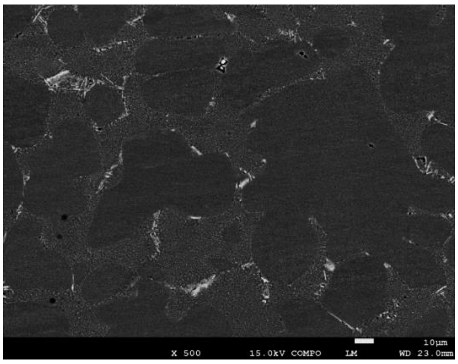

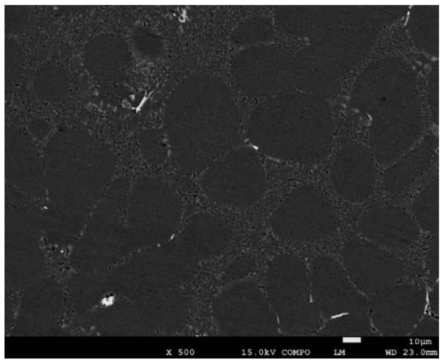

(a) (b)

Figure 27. BSE image of grain refined and modified squeeze cast A356 alloy samples **(a)**A356+Al-5Ti-1B(750ppm Ti and 150ppm B)+Al-10Sr (200ppm Sr) **(b)** A356+Al-5Ti-1B(750ppm Ti and 150ppm B)+Al-10Sr (300ppm Sr)

The volume fraction of Fe based intermetallics (indicated by brighter regions in Fig. 27a) is more in case of alloy having 200ppm Sr than that in alloy having 300ppm Sr. It can be predicted that alloy having high Sr content reduces the modification ability of Sr. It may be due to formation of SrB_6 particles which settle down in the crucible and modification ability of Sr is reduced. Hence in previous research work, the Sr:B ratio which was predicted to be greater than 0.4 for effective Sr modification ability, which is proved to be a wrong statement in current research work

[57]. Further, investigation is required for predicting the range of the ratio for effective modification ability of Sr.

5.5 EDS analysis

5.5.1 EDS layered image /Mapping of A356 alloy

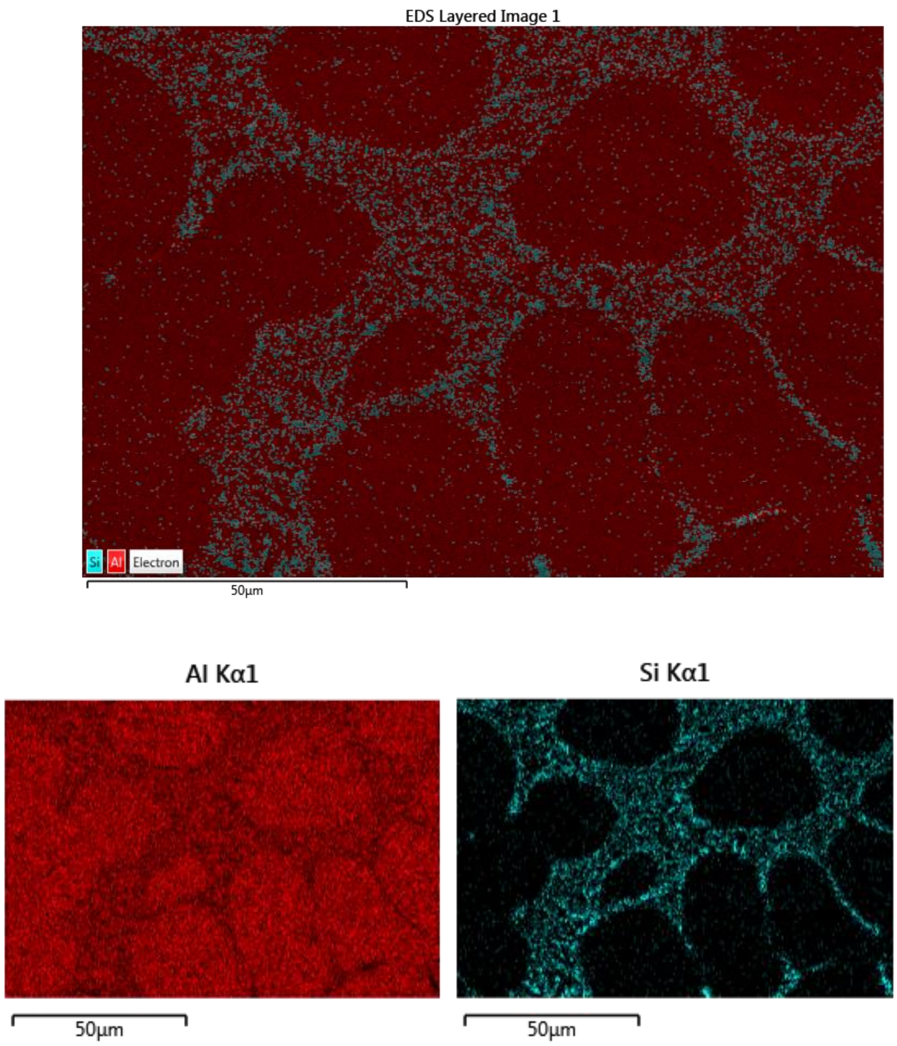

Figure 28. Mapping of A356 alloy indicating α-Al and Si eutectic regions

EDS Layered image shows the location of eutectic Si phase in the inter-dendritic regions of α-Al matrix.

5.5.2 EDS analysis of heat treated squeeze cast A356 alloy

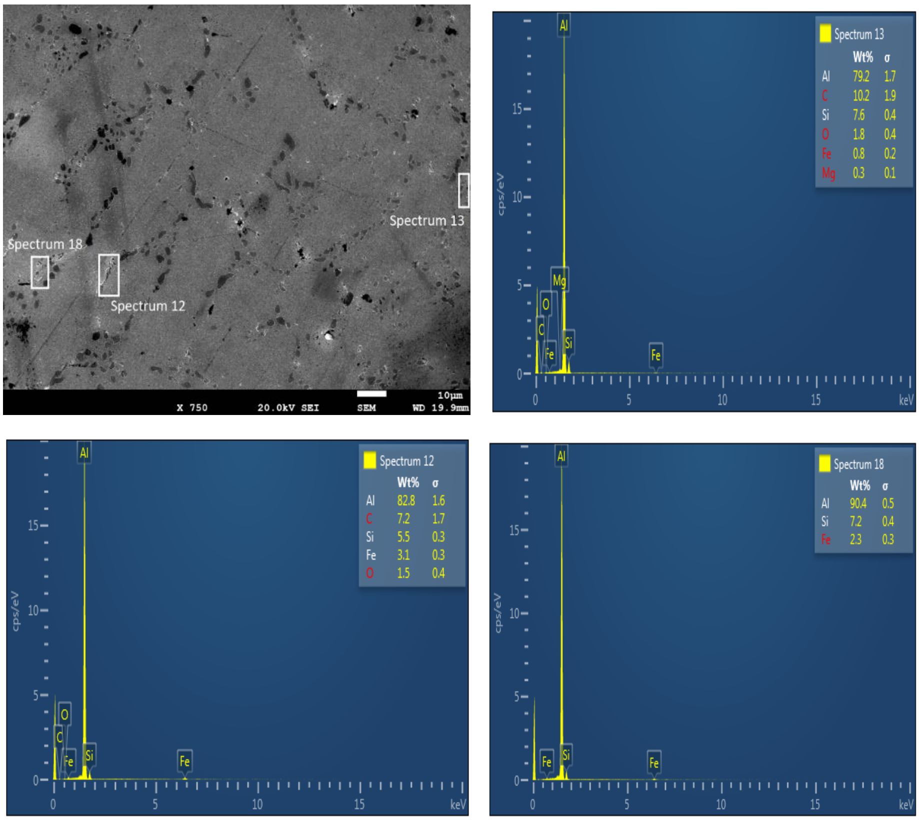

Figure 29. EDS analysis shows the precipitation of Mg_2Si particles and Fe based intermetallics after heat treatment process

The following predictions may be made from EDS analysis of squeeze cast A356 alloy after T6 heat treatment process:

- Precipitation of Al-Si-Fe-Mg phase is observed
- Precipitation of iron based β-intermetallics is observed

5.5.3 EDS analysis of grain refined and modified squeeze cast A356 alloy

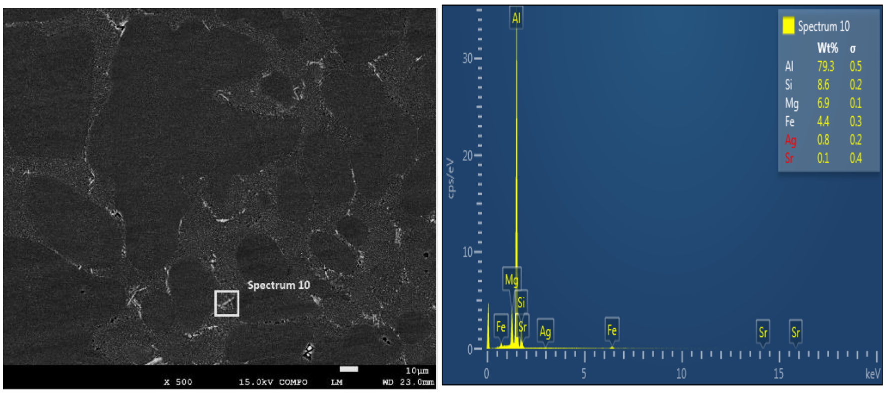

Figure 30. EDS report of grain refined and modified alloy shows the formation of α-phase intermetallic

It was found that the alloy having 200ppm of Sr develops Fe based α-phase intermetallics having Chinese Script morphology in bulk than that in alloy having 300ppm Sr and reduce formation of β-phase intermetallic.

5.6 XRD data analysis

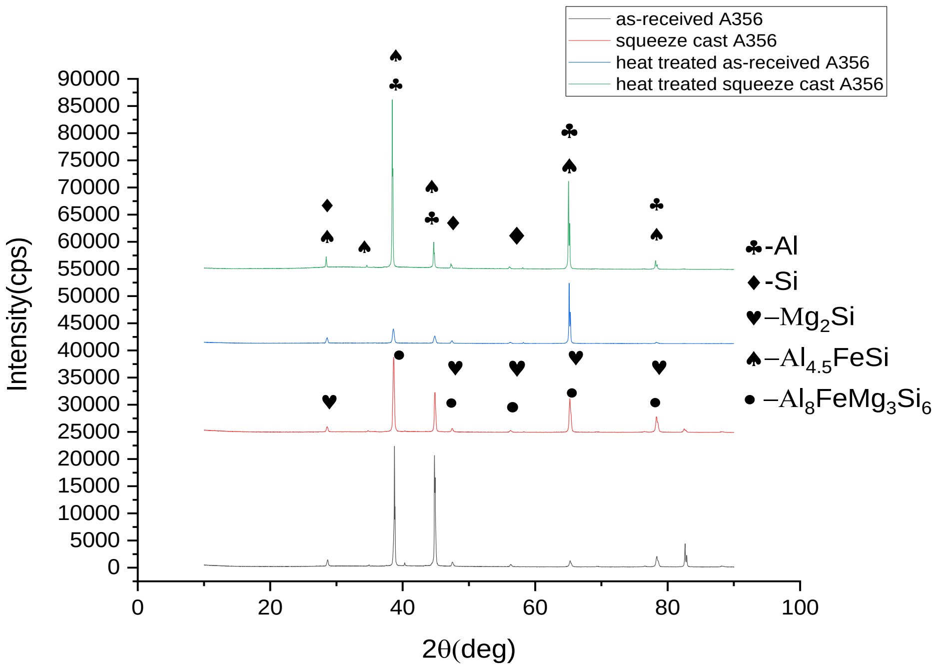

Figure 31. XRD plot of squeeze cast and heat treated samples

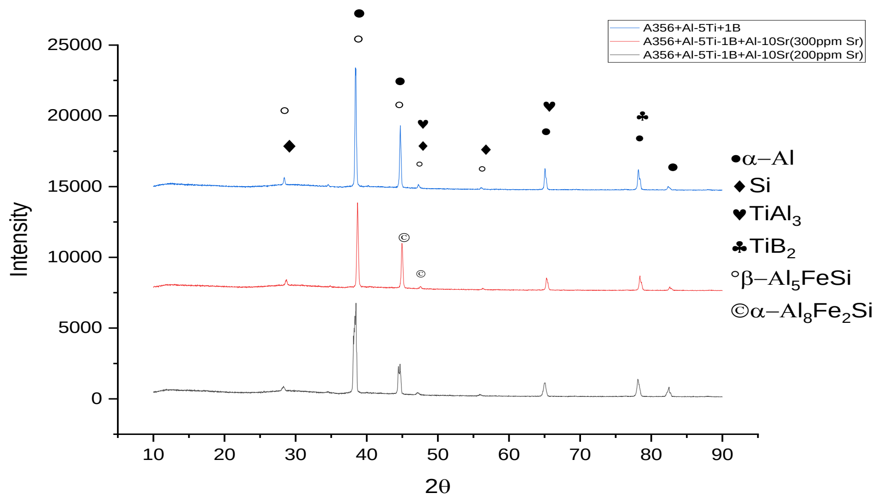

Figure 32. XRD Plot of grain refined and modified squeeze cast samples

From the XRD plot, the transformed phases were observed especially at 39,44,65 and 78 degrees. Similar observations were made by T. Tuncay [98]. The main intermetallic phases detected from XRD Plot for heat treated and non-heat treated samples include Mg_2Si, $Al_{4.5}FeSi$ and $Al_8FeMg_3Si_6$ (Fig. 31). The phases observed from XRD plot for grain refined and modified squeeze cast samples include $TiAl_3$, TiB_2, β-Al_5FeSi and α-Al_8Fe_2Si (Fig. 32).

5.7 Fretting wear analysis

5.7.1 Fretting wear analysis using SEM

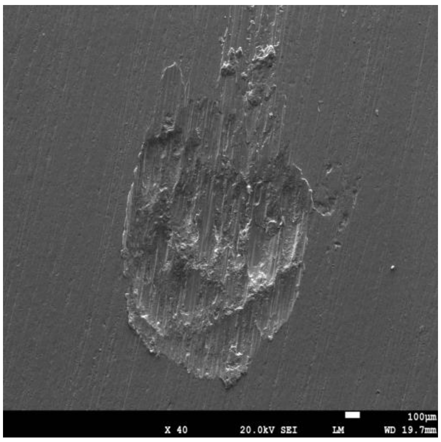

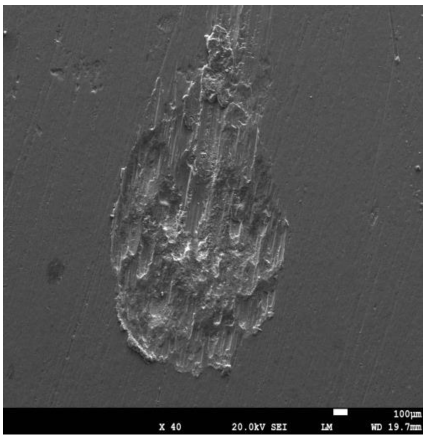

(a) (b)

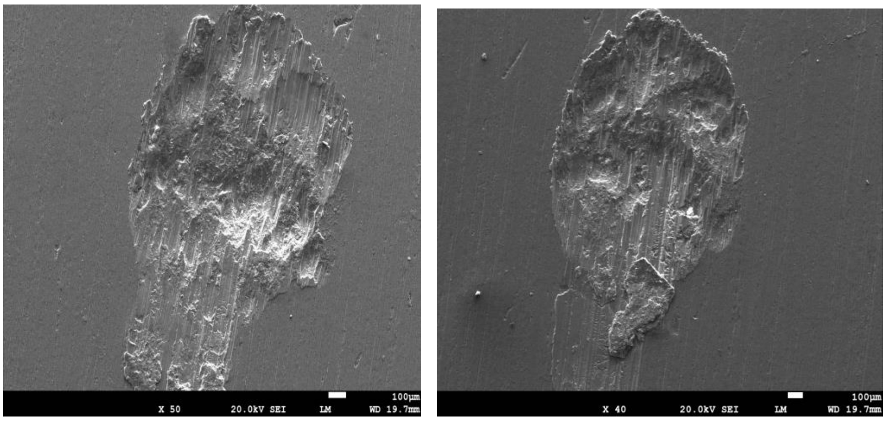

(c) (d)

Figure 33. SEM image of fretting wear scar at various loading conditions (a)5N (b)10N (c)15N (d)20N

Higher wear depth was observed at higher loading conditions.

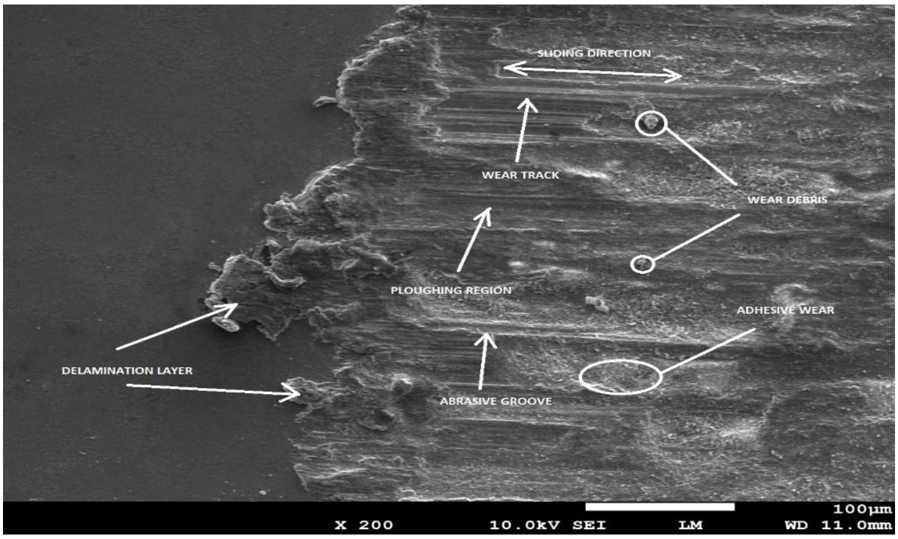

Figure 34. SEM image of fretting wear showing various wear terminologies

5.7.2 EDS layered image or Mapping

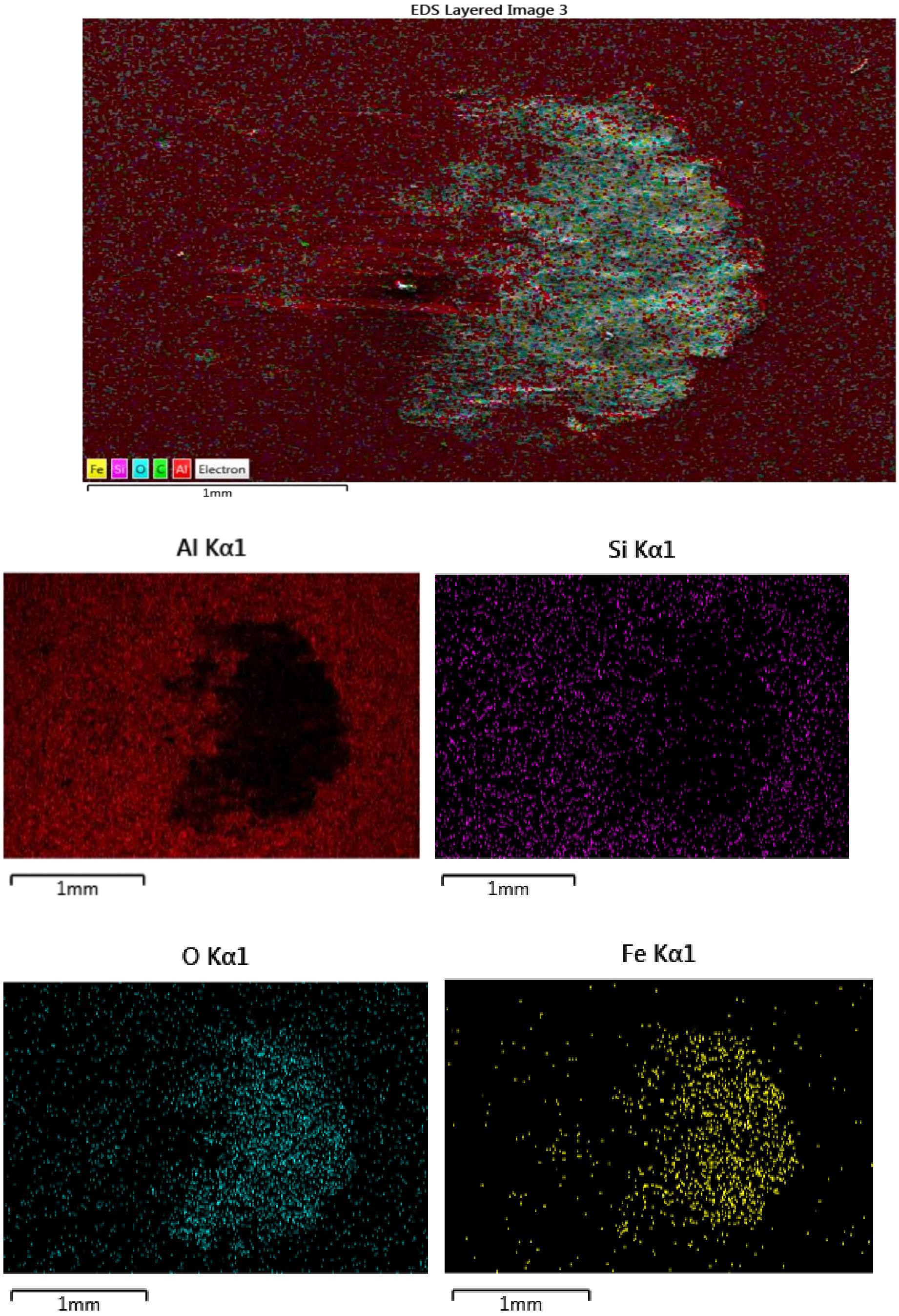

Figure 35. Mapping of fretting wear scar showing presence of various elements

The following observations were made from the EDS analysis:

- The wear debris formed during fretting wear reacts with oxygen present in the atmosphere and forms oxides and hence oxygen content is observed while mapping the specimen under EDS analysis.

- Due to diffusion of particles across the contact surface during fretting wear, some of the Fe particles undergo diffusion from counter specimen i.e. steel to test specimen i.e. Al alloy. Hence Fe content is observed while mapping the test specimen under EDS analysis.

5.7.3 Variation of COF with number of fretting wear cycles for as-received and squeeze cast A356 alloy samples

5.7.3.1 At room temperature

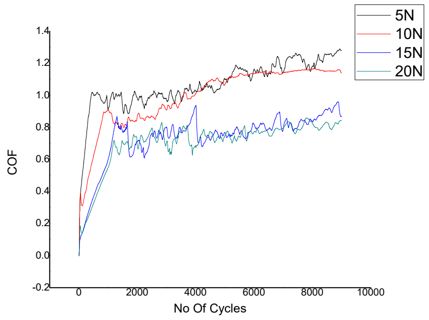

(a)

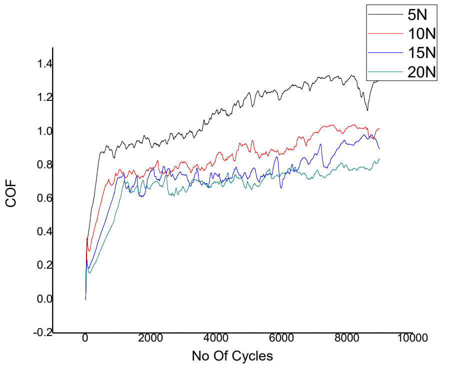

(b)

Figure 36. Variation of coefficient of friction with number of fretting wear cycles for (a)as-received A356 (b)squeeze cast A356 alloy

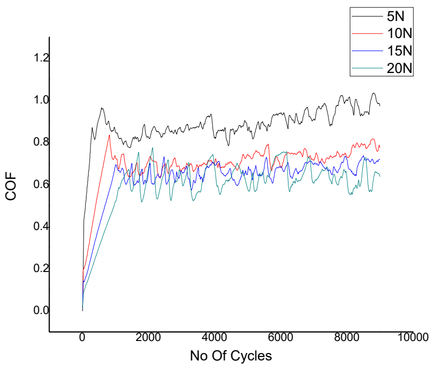

(a)

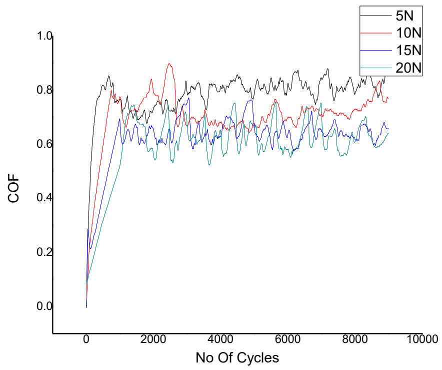

(b)

Figure 37. Variation of coefficient of friction with number of fretting wear cycles for (a)heat treated as-received A356 alloy (b)heat treated squeeze cast A356 alloy

COF decreases with increase in load. COF increases initially due to adhesive and abrasive wear and with increase in number of cycles it attains a steady state due to formation of compact bed of debris which acts as a work hardened layer and decreases abrasive action

5.7.3.2 At elevated temperature of 100°C

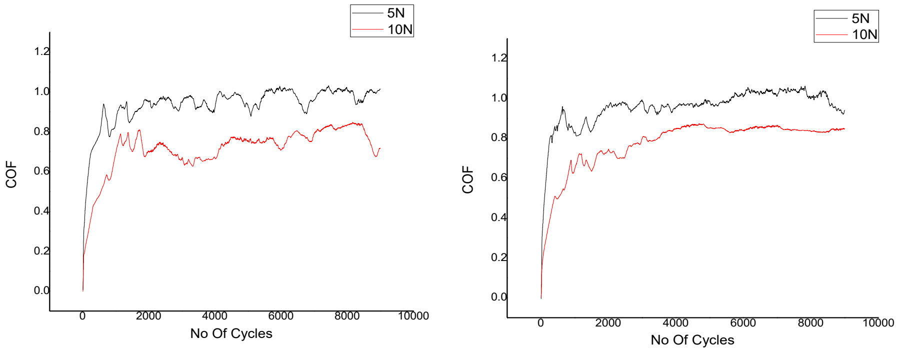

(a) (b)

Figure 38. Variation of coefficient of friction with number of fretting wear cycles for (a)as-received A356 (b)squeeze cast A356 alloy

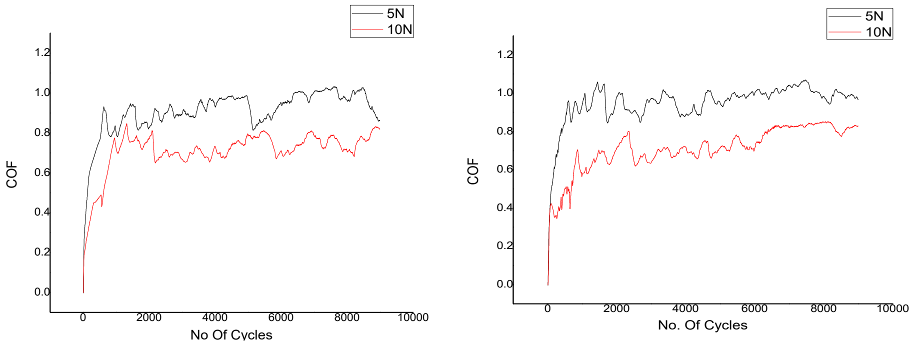

(a) (b)

Figure 39. Variation of coefficient of friction with number of fretting wear cycles for (a)heat treated as-received A356 (b)heat treated squeeze cast A356 alloy

It was observed that at elevated temperature the frictional force declines due to the effect of softening of the mating surface material and decrease in the strength of the adhesive joints. Also, at elevated temperature of 100°C the contact interface area rises, as a result of which large number of adhesive joints become active and friction coefficient increases. Hard oxide debris formed due to oxidation may also increase the COF. Hence.

at elevated temperature, the friction coefficient is neither too high nor too low. However, to find out the relation between apparent contact area and COF under these conditions, further more studies are required for chemical and physical tribology behaviour of the mating surfaces at elevated temperature. Similar predictions were made by Liliyang et al for ball on disc wear test at elevated temperature for Al alloys [99]. The average COF with no, of fretting cycles are shown in Table 3.

Table 3. Variation of COF with normal load applied at room temperature

Load (N)	Friction coefficient of as received A356 alloy	Friction coefficient of Squeeze cast A356 alloy	Friction coefficient of heat treated as received A356	Friction coefficient of heat treated squeeze cast A356
5	1.09	1.07	0.88	0.78
10	0.99	0.84	0.70	0.70
15	0.74	0.74	0.63	0.62
20	0.71	0.67	0.59	0.59

Table 4. Variation of COF with normal load applied at elevated temperature

Load	Friction coefficient of as received A356 at 100°C	Friction coefficient of squeeze cast A356 at 100°C	Friction coefficient of heat treated as received A356 at 100°C	Friction coefficient of heat treated squeeze cast A356 at 100°C
5	0.93	0.95	0.91	0.94
10	0.71	0.77	0.71	0.71

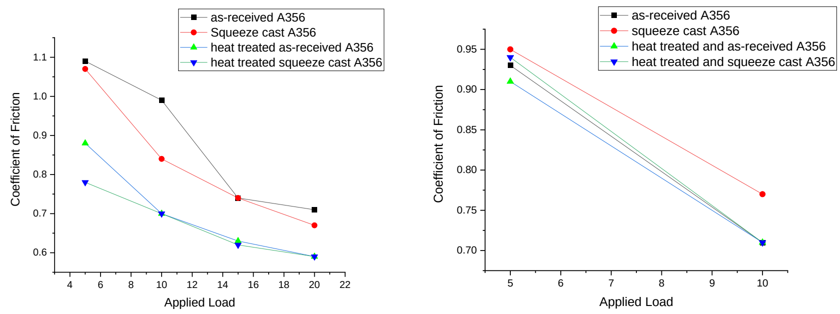

(a) (b)

Figure 40. Variation of coefficient of friction with applied normal load for various samples at (a) room temperature (b) elevated temperature of 100°C

The following predictions may be made after performing the tests:

- Diffusion process is involved in the fretting wear process which cause transfer of materials across the interface of the mating metallic specimens and hence the loss in mass was found to be fluctuating though it was negligible i.e. about 10^{-4} to 10^{-5} grams after fretting wear experiment.
- As coefficient of friction is inverse of hardness in some cases, hence sample having lowest friction coefficient may be considered as the hardest among all specimens. Here, squeeze cast sample undergoing heat treatment can be considered hardest of all samples.

- At elevated temperatures, friction coefficient was observed to be intermediate.

5.7.4 Variation of coefficient of friction with number of fretting wear cycles for grain refined and modified samples

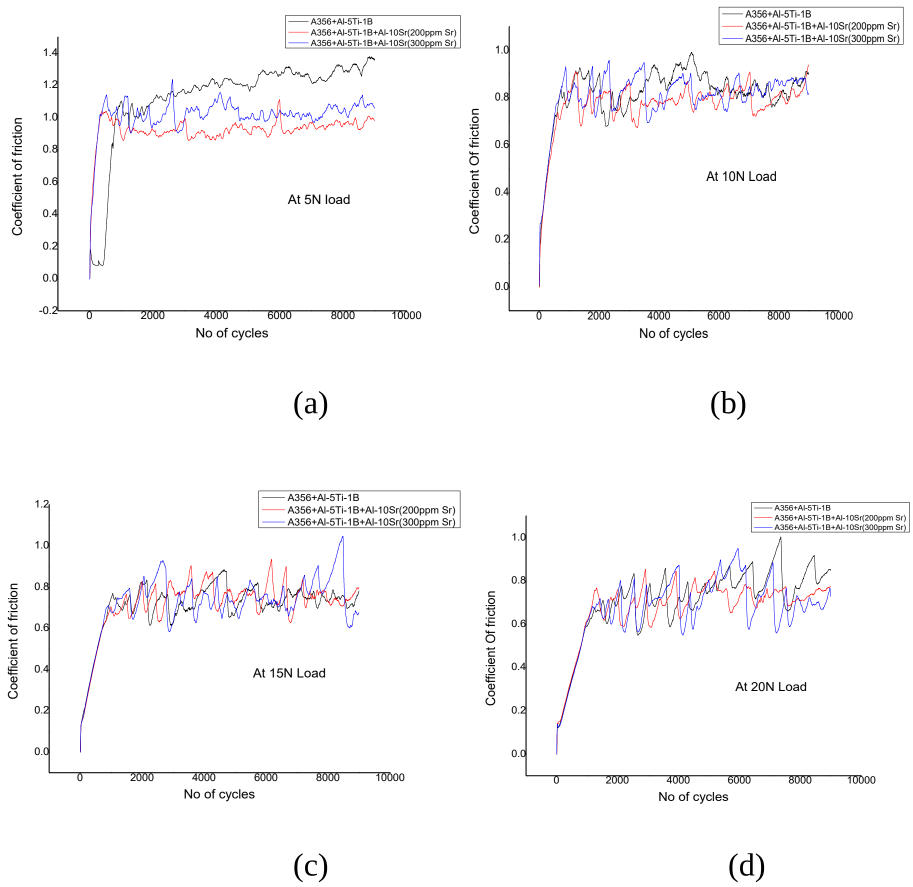

Figure 41. Variation of coefficient of friction with number of fretting cycles for grain refined and modified samples at various loading conditions (a)5N (b)10N (c)15N (d)20N

COF is found to be rising (action of abrasive and adhesive wear) in initial no of cycles and further becomes steady (formation of compact wear debris bed) with the increase in no of fretting wear cycles. The trend of variation of COF with increase in no. of fretting cycles is similar in all the cases (both refined and non-refined alloy)

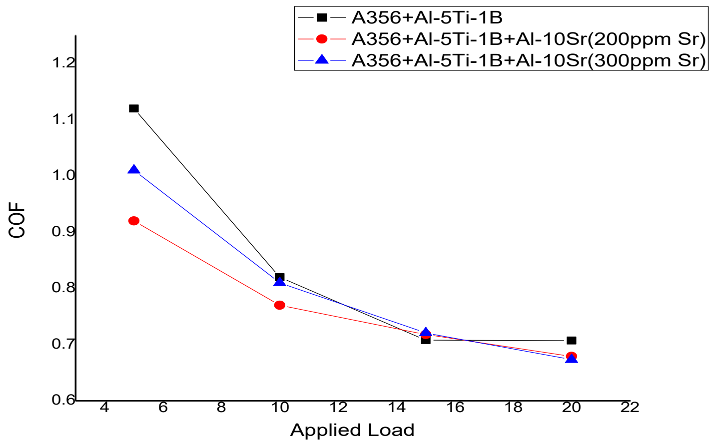

Figure 42. Variation of COF with applied load for grain refined and modified alloy

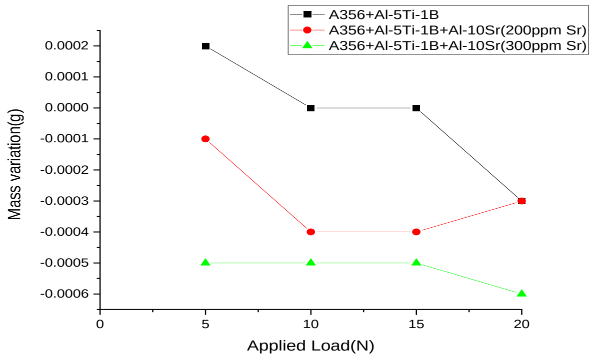

Figure 43. Variation of mass with applied load for grain refined and modified alloy

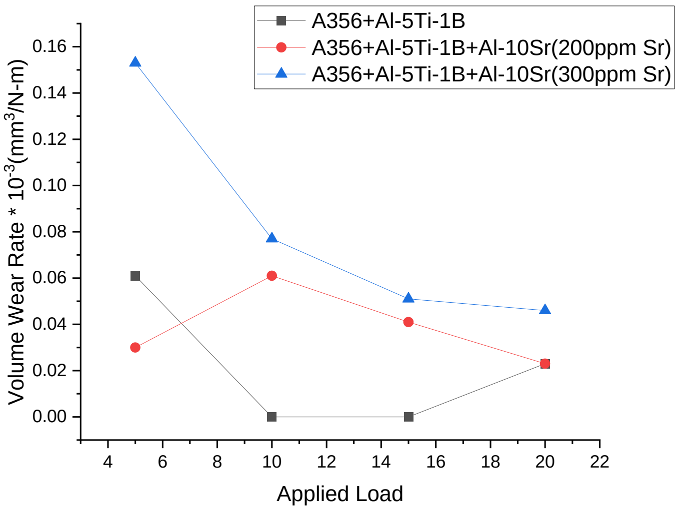

Figure 44. Variation of volume wear rate with applied normal load

$$\text{Volume Wear Rate} = \frac{Volume\ Loss}{Sliding\ Distance \times Applied\ Load} = \frac{Density \times Mass\ Loss}{Sliding\ Distance \times Applied\ Load}$$

COF decreases with increase in load in all the cases. During fretting wear, there is fluctuation in mass of the samples due to material transfer across the interface between counter specimen and the test specimen. The average coefficient of friction of various samples are shown in Table 5.

Table 5. Variation Of COF with load for various sample conditons

Samples	Avg COF at 5N Load	Avg COF at 10N Load	Avg COF at 15N Load	Avg COF at 20N Load
As-received A356	1.09	0.99	0.74	0.71
Squeeze cast A356	1.07	0.84	0.74	0.67
Squeeze cast A356+Al-5Ti-1B	1.12	0.82	0.71	0.707
Squeeze cast A356+Al-5Ti-1B+ Al-10Sr(200ppm Sr) addition	0.92	0.77	0.71	0.679
Squeeze cast A356+Al-5Ti-1B+ Al-10Sr(300ppm Sr) addition	1.01	0.81	0.721	0.673

The following conclusions were made on performing fretting wear tests for grain refined and modified samples:

- It was observed that higher the Sr content (≥ 300ppm Sr), more is the mass loss and volume wear rate. Moreover, it was also observed that the addition of strontium to some optimum level (<300ppm Sr) decreases the coefficient of friction and hence it can be predicted that the hardness of the alloy is increased.
- The COF was found to be higher in case of alloy having 300 ppm of Strontium than that of the alloy having 200ppm Strontium.
- The combined addition of grain refiner and modifier in the form of Al-5Ti-1B and Al-10Sr respectively was found to be effective since the COF got reduced as compared to non-refined and non-modified alloy. Hence it can be predicted that the alloy got hardened after grain refinement and modification using master alloys.
- At higher loading conditions(≥20N), not only hardness affect COF but also shear strength of the adhesive bond between the asperities decides the COF between the surfaces. Further investigation is required for more conclusive results.

Similar predictions were made by N. Arun Prakash et al, D. Arnell, N.M. Mikhin et al for various types of wear tests and at various conditions [100-102].

5.8 Dry sliding wear analysis

In dry sliding wear experiment, it was observed that the average friction coefficient for squeeze cast alloy specimen is lower than that of as-received cast alloy specimen at a sliding velocity (SV) of 0.15m/s and wear track diameter (WTD) of 10 mm (Fig. 45a). But at a SV of 0.25m/s and WTD of 20 mm, the average friction coefficient of squeeze cast specimen was observed to be increasing with sliding time (Fig. 45b). Hence, prediction may be made that the friction coefficient not only depends upon hardness of the sample but also depends upon shear strength of the samples undergoing wear. This was first reported by A.

J. W. Moore et.al. as a general statement for any materials subjecting to dry sliding wear [103]. Similar predictions may be made in case of Al-Si alloy.

Table 6. Dry Sliding Wear test results of all the samples

Testing Parameters	COF of As-received A356	COF of Squeeze cast A356 COF	As-received A356 Wear(micron)	Squeeze cast A356 Wear(micron)
SV-0.15,WTD-10mm	0.269	0.199	156.317	80.494
SV-0.25,WTD-20mm	0.303	0.375	246.569	119.158

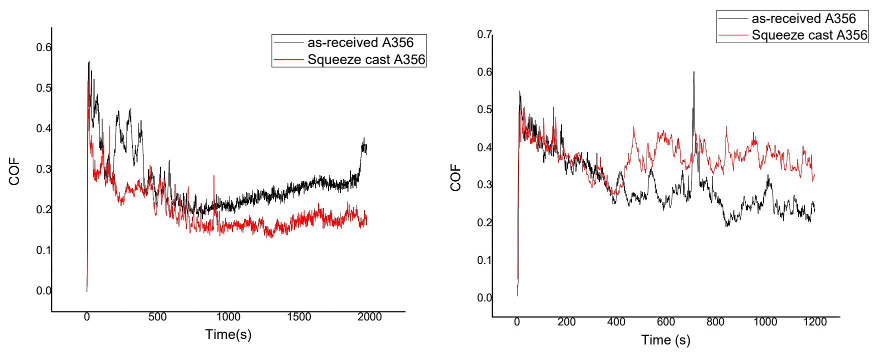

(a) (b)

Figure 45. COF v/s sliding time for SV of (a) 0.15 m/s (b) 0.25 m/s

Moreover, the depth of wear for squeeze cast alloy specimen was observed to be lower than that of as-received alloy specimen (See Table 6) and hence, predictions may be made that the hardness of the material got improved on using squeeze casting process.

Further, more investigations are required to obtain more conclusive results.

Chapter 6

Conclusions

The following conclusions were drawn from the research work in this study :

- In A356 alloy, a significant reduction in secondary dendrite arm spacing from as-received A356 alloy having SDAS of 45(+/- 2) μm to squeeze cast A356 alloy having SDAS of 26 (+/- 2) μm was observed after squeeze casting process. Moreover, refinement of Si eutectic region was also observed in squeeze cast A356 alloy samples.
- In heat treated squeeze cast A356 alloy, the T6 heat treatment process was found to be more effective due to uniform precipitation of intermetallics including Mg_2Si in the interdendritic regions of α-Al matrix accompanied with change in the morphology of Si particles.
- In squeeze cast A356+ Al-5Ti-1B alloy, a significant reduction in secondary dendrite arm spacing from as-received A356 alloy having SDAS of 45 (+/- 2) μm to grain refined alloy having SDAS of 20 (+/-3) μm. Moreover, the morphology of α-Al phase was observed to change from dendritic to globular shape.
- In squeeze cast A356 + Al-5Ti-1B + Al-10Sr (200ppm Sr) alloy, the reduction of secondary dendrite arm spacing was observed from as-received A356 alloy having SDAS of 45(+/- 2) μm to grain refined and modified alloy using 200ppm Sr having SDAS of 20(+/-3) μm. Whereas, in squeeze cast A356 + Al-5Ti-1B + Al-10Sr (300ppm Sr), the secondary dendrite arm spacing was observed to be 20 (+/- 2) μm. There is not much change in SDAS with addition of Al-10Sr alloy or varying the composition of Sr because Sr is only responsible for changing the morphology of Si particles and iron based intermetallics.

- In squeeze cast A356 + Al-5Ti-1B + Al-10Sr alloy, iron based α-intermetallics having Chinese script morphology were observed while morphology of Si particles changed from needle shaped to fine fibrous/globular shaped.
- In heat treated squeeze cast A356 + Al-5Ti-1B alloy, heat treatment was found to be effective due to uniform distribution of precipitates within the matrix of α-Al phase and also at interdendritic regions of α-Al matrix
- In heat treated squeeze cast A356 +Al-5Ti-1B +Al-10Sr alloy, heat treatment was not effective due to reduced precipitation effect.
- In A356 alloy, the microstructural images using SEM indicates the absence of microporosities after squeeze casting process. Moreover, the Si particles were found to be broken into small fragments after squeeze casting process.
- In heat treated squeeze cast A356 alloy, the SEM images shows that the morphology of Si particles changed from needle shape morphology to spheroidal shape morphology.
- In squeeze cast A356 +Al-5Ti-1B +Al-10Sr alloy, the microstructural images using SEM indicate the presence of lamellar Si particles in some locations of the Al-Si eutectic region which depicts partial modification of the alloy on addition of Sr as a modifying agent. This might be due to lack of Sr content or Sr content was insufficient in those regions for modification of Si particles.
- In squeeze cast A356 + Al-5Ti-1B + Al-10Sr (200 ppm Sr) alloy, the SEM analysis using BSE imaging indicates that the volume fraction of Fe based intermetallics is more than that of squeeze cast A356 + Al-5Ti-1B + Al-10Sr (300ppm Sr) alloy. This might be due to reaction between Sr and B to form SrB_6 particles which settle down in the crucible thereby reducing the modification ability of Sr when higher Sr content is added.

- In heat treated squeeze cast A356 alloy, the EDS analysis indicates the precipitation of Al-Fe-Mg-Si precipitates and iron based β- intermetallics.
- In fretting wear tests for all the samples of A356 alloy, the SEM images of wear scars indicates that the wear depth increases with increase in applied load. Moreover, the EDS mapping of fretting wear samples indicates the presence of oxides due to formation of oxide debris and also indicates the presence of Fe due to diffusion of Fe particles across the contact surface from counter specimen i.e. steel to test specimen i.e. A356 alloy. Hence, fluctuations in mass of the specimen was observed after each fretting wear tests performed.
- In fretting wear tests for all the samples of A356 alloy, it was observed that the coefficient of friction decreases with increase in applied normal load. Moreover, the variation of coefficient of friction with increase in number of fretting cycles was found to be increasing initially due to adhesive and abrasive wear, followed by steady state variation in coefficient of friction due to formation of a compact bed of oxide wear debris which acts as work hardened layer and decreases the abrasive action of the wear.
- In fretting wear tests at elevated temperature of 100°C, there is an increment in coefficient of friction due to increase in number of adhesive joints and formation of oxide debris. Moreover, the softening of the mating surface weakens the strength of adhesive joints which in turn decreases the friction coefficient. Hence, the coefficient of friction at elevated temperature is neither too low nor too high.
- In squeeze cast A356 +Al-5Ti-1B+Al-10Sr (300ppm Sr) alloy, the mass loss was found to be maximum and high volume wear rate. Hence Sr content higher than 300ppm is not acceptable.
- In squeeze cast A356 +Al-5Ti-1B +Al-10Sr (200ppm Sr) alloy, the coefficient of friction was found to be lower than that of

squeeze cast A356 +Al-5Ti-1B +Al-10Sr (300ppm Sr) alloy. Hence it can be predicted that the alloy having 200ppm of Sr is harder than that of alloy having 300ppm of Sr.

- The combined addition of grain refiner Al-5Ti-1B and grain modifier Al-10Sr to squeeze cast A356 alloy was found to be effective as the values of coefficient of friction was found to be lower than that of non refined and non modified squeeze cast A356 alloy. Hence, it can be predicted that the grain refiner and grain modifier had hardened the alloy significantly. Moreover, at higher loading conditions (>20N), it is not only the hardness that affects the coefficient of friction but also the shear strength of the adhesive bond between asperities decides the coefficient of friction between the mating surfaces. Further investigations are required for more conclusive results.
- In dry sliding wear tests, it was observed that the depth of wear for squeeze cast A356 alloy samples were lower than that of as-received A356 alloy samples. Hence it can be predicted that the A356 alloy sample got hardened after squeeze casting process. Moreover, the variation in coefficient of friction with sliding time was observed to be contradictory after changing the wear parameters. Hence further investigations are required to obtain more conclusive results.

Chapter 7

Future Scope

7.1 Squeeze casting pressure

The study of Si based Al alloy will continue with the development of new processing technologies for improving the mechanical properties of the alloy. It is believed that Al-Si alloys can be further grain refined and modified by increasing the pressure during squeeze casting process. Hence further research can be done to identify the optimum pressure required to obtain better mechanical properties

7.2 Alloy development

Since it is observed that the addition of master alloys can modify the microstructural and mechanical properties of the alloy, hence further more investigations can be done by varying the compositions of the master alloy addition to obtain optimum range of addition of master alloy for maximum improvement in mechanical properties.

7.3 Heat treatment

As it is well known that precipitation hardening is one of the major strengthening mechanism to improve the strength of an alloy. Since Al-Si alloy is heat treatable alloy, further more attempts can be done by varying the solutionizing temperature, aging temperature, soaking temperature and time to obtain better results as far as strength of the alloy is concerned.

7.4 Mechanical properties

The mechanical properties like strength, hardness, toughness, ductility etc under static loading conditions can be further investigated.

Several cast Al alloy components are subjected to cyclic loads during their operation and hence it is interesting to investigate the dynamic mechanical properties of the alloy. Thus the role of SDAS and morphology of Si on fatigue behaviour of Si based Al alloys can be investigated.

Moreover, from corrosion point of view, Si particles are cathodic in nature as compared to α-Al matrix and hence form micro galvanic couples which results in localised corrosion phenomena. But Al-Si alloy is still considered to have good corrosion resistant property than that of other conventional alloys. Hence the study of corrosion resistant property of Al-Si alloys can be done.

In most of the industrial applications the components operate at elevated temperature and hence the behaviour of Al-Si alloy at elevated temperature can be studied as far as mechanical properties like strength, ductility, toughness, hardness and wear properties are concerned.

REFERENCES

1. Davis J.R. (1993), editor. ASM Specialty Handbook: Aluminium and Aluminium Alloys. ASM International .
2. Mondolfo LF. (1976), Aluminum alloys, structure and properties. London, Butterworths and Co. Ltd..
3. Haizhi Ye (2003). An overview of the development of Al–Si-alloy based material for engine applications. J Mater Eng Perform 12:288–97.
4. Eklund JE. (1993), On the effects of impurities on solidification and mechanical behavior of primary and secondary commercial purity aluminum and aluminum alloys, PhD. thesis. Helsinki: University of Technology.
5. Taylor JA, Schaffer GB, St John DH (1999), The role of iron in the formation of porosity in Al–Si–Cu-based casting alloys. Metall Mater Trans 30A:1643–62.
6. Suárez-Peña B, Asensio-Lozano J.(2006), Influence of Sr modification and Ti grain refinement on the morphology of Fe-rich precipitates in eutectic Al–Si die cast alloys. Scripta Mater 54:1543–8.
7. Kori S.A., Murty B.S., Chakraborty M. (2000), Development of an efficient grain refiner for Al-7Si alloy and its modification with strontium, Mater. Sci. Eng. A. 283, 94-104.
8. Prasada Rao A.K., Das K., Murty B.S., Chakraborty M.(2008), Microstructure features of as-cast A356 alloy inoculated with Sr, Sb, modifiers and Al-Ti-C grain refiner simultaneously, Mater. Lett. 62, 273-275
9. Barrirero J., Li J.H., Engstler M., Ghafoor N., Schumacher P., Odén M., Mücklich F. (2016), Cluster formation at the Si/liquid interface in Sr and Na modified Al–Si alloys, Scripta Mater. 117, 16-19
10. Li J.H., Albu M., Hofer F., Schumacher P. (2015), Solute adsorption and entrapment during eutectic Si growth in A–Si-based alloys, Acta Mater. 83, 187-202

11. Closset, B., Drew, R.A.L., and Gruzleski, J.E., (1986). Eutectic Silicon Shape Control by In Situ Measurement of Electrical Resistivity, Transactions of the American Foundrymens Society, 94,9-16
12. Shivkumar, S., Ricci, S., Steenhoff, B., Apelian, D., and Sigworth, G., (1989). An. Experimental Study to Optimize the Heat Treatment of A356 Alloy, Transactions of the American Foundrymens Society, 97, 791-810.
13. Zhang, D.L., Zheng, L.H., and St John, D.H., (2002). Effect of a short solution treatment time on microstructure and mechanical properties of modified Al-7wt.%Si-0.3wt.%Mg alloy. Journal of Light Metals, 2 (1), pp.27-36
14. Guinier A.(1959), Solid State Physics 9, 293
15. Bagaryatsky Y.A., Dokl. Akad. Nauk (1952) SSSR 87, 559
16. Couture A.(1981), Iron in aluminum casting alloys: a literature survey. AFS Int Cast Metals J,6:9–17
17. Chernov D.K.(1878), Reports of the Imperial Russian Metallurgical Society, Dec.
18. Welter V.G., Metallkd Z.(1931), 23, 255.
19. Chatterjee S. and Das A.A.(1973). Some observations on the effect of pressure on the solidification of Al-Si eutectic alloys. British Foundryman, 66.
20. Chatterjee S. and Das A.A.,(1972), Effects of pressure on the solidification of some commercial aluminium base casting alloys. British Foundryman, 65
21. Chadwick G.A. and Yue T.M.,(1989), Principles and applications of squeeze casting. Metals and Materials
22. Dong J.X., Karnezis P.A., Durrant G., and Cantor B. (1999). The effect of sr and fe additions on the microstructure and mechanical properties of a direct squeeze cast Al-7Si-0.3Mg alloy. Metallurgical and Materials Transactions A, 30A: 1341-1356

23. Okada S., Fuji N., Goto A., Morimoto S., and Yasuda T.(1982), Development of a fully automatic squeeze casting machine. AFS Transactions, 82(16).
24. Fredriksson H., Åkerlind U.(2001), Solidification and Crystallization Processing in Metals and Alloys, John Wiley & Sons Ltd., Chichester, 2012M. Makhlouf, H. Guthy, Journal of Light Metals, 1 199-218.
25. Backerud L., Chai G. and Tamminen J.(1990): 'Solidification characteristics of aluminum alloys', 2-Foundry Alloys, Skan Aluminum, USA, 115–150.
26. Sritharan T., Li H.(1997), Influence of Titanium to Boron Ratio on the Ability to Grain Refine Aluminium-Silicon Alloys, Journal of Materials Processing Technology 63,585-589
27. Jones G.P., Pearson J.(1976), Factors Affecting Grain Refinement of Aluminium using Ti and B Additives, Metal!. Trans. 7B, 223-234
28. Mayes C.D., McCartney D.G., Tatlock G.J.(1993), Influence of Microstructure on Grain Refining Performance of Al-Ti-B Master Alloys, Mater. Sci. Techno!. 9,97-103
29. Mohanty P.S. and Gruzleski J.E.(1996), "Grain refinement mechanisms of hypoeutectic Al-Si alloys", Acta Materialia, 44 ,3749-3760.
30. Spittle J.(2006), "Grain refinement in shape casting of aluminium alloys", International Journal of Cast Metals Research, 19 (4), 210-222
31. Schumacher P.(2003), "Nucleation Mechanisms during Grain Refinement of Al-Si-Alloys" (in German), Giesserei-Rundschau, 50 ,228-230.
32. Mohanty P.S., Samuel F.H., Gruzleski G.E.,(1995), Metall. Trans. B 26,103.
33. Ghomashchi R.(2012), "The evolution of AlTiSi intermetallic phases in Ti-added A356 Al-Si alloy", Journal of Alloys and Compounds, 537 , 255-260.

34. Sigworth G. und Guzowski M.,(1985), Grain Refining of Hypoeutectic Al-Si Alloys, AFS Transactions, 907-912.
35. Tøndel P.A., Halvorsen G. and Arnberg L.,(1992), "Grain refinement of hypoeutectic Al-Si foundry alloys by addition of boron containing silicon metal", Light Metals 1993, ed. S.K. Das (Denver, CO: TMS), 783-789
36. Nafisi S. and Ghomashchi R.(2007), "Boron-based refiners: Implications in conventional casting of Al-Si alloys", Materials Science and Engineering A, 452-453 , 445-453
37. Birol Y.,(2012), "Performance of AlTi5B1, AlTi3B3 and AlB3 master alloys in refining grain structure of aluminium foundry alloys", Materials Science and Technology, 28 (4) 481-486
38. Sigworth G.,(1984), The Grain Refining of Aluminium and Phase Relationships in the Al-Ti-B System, Metallurgical Transactions A, 15 , 277-282
39. Sebastian F. Fischer, Roman Boras, Andreas Bührig-Polaczek, Matthias Bünck,(2014) Efficient Use of Titanium and Boron in Grain Refining of a Die-cast Strontium-modified A356, Shape Casting: 5th International Symposium.
40. Lu H.T., Wang L.C., S.K. and Kung,(1981), "Grain Refining in A356 Alloys, J. Chinese Foundrymen's Association, Vol. 29, pp. 10–18
41. Sigworth GK.(2014), Fundamentals of Solidification in Aluminum Castings. Int J Metalcasting;8(1):7–20.
42. Bäckerud L, Gustafson P, Johnsson M.,(1991), Grain refining mechanisms in aluminum as a result of additions of titanium and boron, part II. Aluminium. 67:910–915.
43. Davies IG, Dennis JM, Hellawell A.,(1970) The nucleation of aluminum grains in alloys of aluminum with titanium and boron. Metallurgical Transactions. Vol. 1.,p. 275–279.
44. Maxwell I, Hellawell A.,(1975), A simple model for grain refinement during Solidification. Acta Metallurgica.23:229–237.

45. Choongdo Lee,(2016), Effect of Ti-B addition on the variation of microporosity and tensile properties of A356 aluminium alloys, 668,152–159
46. Birol Y.(2012), “Grain refinement of pure aluminium and Al-7Si with Al-3B master alloy”, Materials Science and Technology, 28 (3), 363-367.
47. W. Meyer,(1978), Aluminium 54,700.
48. Couture A.,(1981) Iron in aluminum casting alloys: a literature survey. AFS Int Cast Metals J,6:9–17.
49. Kori S.A., Auradi V., Murty B.S., Chakraborty M.,(2005), Poisoning and Fading Mechanism of Grain Refinement in AI-7Si Alloy, Materials Forum Volume 29,387-393
50. Sergio Haro-Rodríguez et al.,(2011), On influence of Ti and Sr on microstructure, mechanical properties and quality index of cast eutectic Al–Si–Mg alloy, 32 ,1865–1871
51. Crosley P.E., Mondolfo L.F.,(1966), The modification of aluminum–silicon alloys, AFS Trans. 74, 53–64.
52. Lu S.Z. and Hellawell A.,(1987), “The Mechanism of Silicon Modification in Aluminum-Silicon Alloys: Impurity Induced Twinning”, Metallurgical Transactions A, 18 ,1721-1733
53. Kori S.A., Auradi V., Murty B.S., Chakraborty M.,(2005), Poisoning and Fading Mechanism of Grain Refinement in AI-7Si Alloy, Materials Forum Volume 29, 387-393
54. Qiu D., Taylor A., Zhang M.X., Kelly P.M.,(2007), A Mechanism for the Poisoning Effect of Silicon on the Grain Refinement of AlSi Alloys, Acta Materialia 55, 1447-1456
55. Hengcheng Liao, Guoxiong Sun,(2003), Mutual poisoning effect between Sr and B in Al–Si casting alloys, 48,1035–1039
56. Timpel M., Wanderka N., Schlesiger R.,Yamamoto T., Lazarev N., Isheim D., Schmitz G.,Matsumura S. and Banhart J.,(2012), “The role of strontium in modifying aluminium-silicon alloys”, Acta Materialia, 60 , 3920-3928

57. Nogita K., McDonald S.D. and Dahle A.K.,(2003), “Effects of Boron-strontium Interactions on Eutectic Modification in Al-10mass%Si Alloys”, Materials Transactions, 44 (4), 692-695
58. Ma Z., Samuel E., Mohamed A.M.A., Samuel A.M., Samuel F.H., Doty H.W.,(2010), Influence of aging treatments and alloying additives on the hardness of Al–11Si–2.5Cu–Mg alloys, Mater. Des. 31 (8) 3791–3803.
59. Ma Z., Samuel E., Mohamed A,M,A, Samuel A.M., Samuel F.H., Doty H.W.,(2010), Parameters controlling the microstructure of Al–11Si–2.5Cu–Mg alloys, Mater. Des. 31 (2) 902–912.
60. Shivkumar S., Ricci Jr. S., Steenhoff B., Apelian D., Sigworth G.,(1989), An experimental study to optimize the heat treatment of A356 alloy, AFS Trans. 97,791–810.
61. Wan Li, Luo Ji-rong, Lan Guo-dong, Liang Qiong-hua,(2008). Mechanical properties and microstructures of squeezed and cast hypereutectic A390 alloy [J]. Journal of Huazhong University of Science and Technology: Natural Science Edition, 36(8): 92-95. (in Chinese)
62. Zhang D L, Zheng L H, Stjohn D H.,(2002) Effect of a short solution treatment time on microstructure and mechanical properties of modified Al-7wt.%Si-0.3wt.%Mg alloy [J]. J Light Metals, 2(1): 27-36.
63. Yu Z, Zhang H , Sun B, Shao G.,(2009) Optimization of soaking time for T6 treatment of aluminium alloy [J]. Heat Treatment, 24(5): 17-20. (in Chinese)
64. Estey C M, Cockcroft S L, Maijer D M, Hermesmann C.,(2004) Constitutive behavior of A356 during the quenching operation [J]. Mater Sci Eng A, 383(2): 245-251
65. Rometsch P A, Schaffer G B.,(2002) An age hardening model for Al-7Si-Mg casting alloys [J]. Mater Sci Eng A, 325(1-2): 424-434
66. Hoeppner D.W., Chandrasekaran V. and Elliot C.B.,(2000), eds. Fretting- fatigue: Current Technologies and Practices, ASTM

STP 1367 (American Society for Testing and Materials, West Conshohocken)

67. Attia M.H. and Waterhouse, R.B.,(1992), eds. Standardization of Fretting Fatigue Test Methods and Equipment, ASTM STP 1159 (American Society for Testing and Materials, Philadelphia).
68. Dobromirski J.M.,(1992), in: Standardization of Fretting Fatigue Test Methods and Equipment, ASTM STP 1159, eds. M.H. Attia and R.B. Waterhouse, (American Society for Testing and Materials, Philadelphia) p. 115
69. Nix K.J. and Lindley T.C.,(1988), Wear 125, 147.
70. Nix K.J. and Lindley T.C.,(1985), Fatigue Fract. Eng. 8 ,143.
71. Venkatesh T.A., Conner B.P., Lee C.S., Giannakopolos A.E., Lindley T.C. and Suresh S.,(2001), Metall. Mater. Trans. A 32, 1131.
72. Chen G.X., Zhou Z.R.,(2001), Wear 250, 665.
73. Berthier Y., Vincent L., Godet M.,(1988), Wear 125,25.
74. Hurricks P.L.,(1970), Wear 15, 389.
75. Waterhouse R.B., Taylor D.E.,(1974), Wear 29,337.
76. Iwabuchi A.,(1991), Wear 151, 301.
77. Okabayashi K., Nakatani Y., Notani H. and Kawamoto M., Keikinzoku,(1964), 14,57
78. Shivanath R., Sengupta P.K. and Eyre T.S.,(1977), Br. Foundryman, 70, 349.
79. Clarke J., Sarkar A.D.,(1979), Wear characteristics of as-cast binary aluminium silicon alloys, Wear, 54, 7 - 16
80. Clarke J., Sarkar A.D.,(1980), Friction and wear of aluminium-silicon alloys, Wear, 61,157 - 167
81. Dewhirst E.V.,(1966), Br. Foundryman, 59, 1.
82. Vandelli G.,(1968), Allum. Nuoua Metall., 37,121.
83. Okabayashi K. and Kawamoto M.(1966), Bull. Univ. Osaka, Prefect., Ser. A, 15,153.
84. Okabayashi K. and Kawamoto M.(1968), Bull. Univ. Osaka, Prefect., Ser. A, 17 199.

85. Pramila Bai B.N., Biswas S.K.(1987), Characterization of dry sliding wear of ai-si alloys, Wear, 120,61- 74
86. Razavizadeh K.and Eyre T.S.(1982), Wear, 79, 325.
87. Razavizadeh K.and Eyre T.S.(1983), Wear, 87 261.
88. Antoniou R. and Borland D.W.,(1987), Mater. Sci. Eng., 93, 57.
89. Pramila Bai B.N. and Biswas S.K.(1991), Acta Mekzll., 39 (5) 833
90. Sarkar A.D.,(1976), "Wear of metals" (Pergamon Press,) p, 86.
91. Mohammed Jasim K.,(1983), MSc thesis, University of Technology, Baghdad.
92. Biswas S.K. and Parmila Bai B.N.(1981), Wear 68,347.
93. Saka N., Eleiche A.M.and Suh N.P.(1977), ibid. 44,109.
94. Suh N.P.(1977), ibid. 44,1.
95. Mohammed Jasim K., Dwarakadasa E.S.(1993), Effect of sliding speed on adhesive wear of binary AI-Si alloys, Journal of materials science letters 12,650-653
96. Subramanain C.,(1991), Effect of sliding speed on unlubricated wear behaviour of Al–12.3% Si alloys.WeaR,151:97–110.
97. Abou El-khair M.T.(2005), Microstructure characterization and tensile properties of squeeze-cast AlSiMg alloys, Materials Letters 59,894– 900
98. Tunçay T.(2017), The Effect of Modification and Grain Refining on the Microstructure and Mechanical Properties of A356 Alloy, Acta Physica Polonica, Vol. 131
99. Liliang Wang, Jingqi Cai, Jie Zhou, Jurek Duszczyk,(2009) Characteristics of the Friction Between Aluminium and Steel at Elevated Temperatures During Ball-on-Disc Tests, Tribol Lett 36:183–190
100. Arun Prakash N., Gnanamoorthy R., Kamaraj M.(2012), Fretting wear behavior of controlled ball impact treated aluminium alloy under dry sliding condition, Surface & Coatings Technology 207, 450–460
101. Arnell D., Mechanisms and laws of friction and wear ,D. Arnell, University of Central Lancashire, UK

102. Mikhin, N.M., Lyapin, K.S.,(1970) Hardness dependence of the coefficient of friction. Soviet Physics Journal 13, 317–321

103. Moore A.J.W., Tegart W.J.M., Bowden, F. P.(1952): Relation between friction and hardness, Proceedings of the Royal Society of London, Series A, Mathematical and Physical Sciences, 212(1111), 452–458.